Persistent neural states: stationary localized activity patterns in nonlinear continuous n-population, q-dimensional neural networks

Olivier Faugeras [a,*], Romain Veltz [a], François Grimbert [a],

[a] *INRIA/ENS/ENPC, Odyssée Team, 2004 route des Lucioles, Sophia-Antipolis, France*

Abstract

Neural continuum networks are an important aspect of the modeling of macroscopic parts of the cortex. Two classes of such networks are considered: voltage- and activity-based. In both cases our networks contain an arbitrary number, n, of interacting neuron populations. Spatial non-symmetric connectivity functions represent cortico-cortical, local, connections, external inputs represent non-local connections. Sigmoidal nonlinearities model the relationship between (average) membrane potential and activity. Departing from most of the previous work in this area we do not assume the nonlinearity to be singular, i.e., represented by the discontinuous Heaviside function. Another important difference with previous work is our relaxing of the assumption that the domain of definition where we study these networks is infinite, i.e. equal to $\mathbb{R}$ or $\mathbb{R}^2$. We explicitely consider the biologically more relevant case of a bounded subset Ω of $\mathbb{R}^q$, $q = 1, 2, 3$, a better model of a piece of cortex. The time behaviour of these networks is described by systems of integro-differential equations. Using methods of functional analysis, we study the existence and uniqueness of a stationary, i.e., time-independent, solution of these equations in the case of a stationary input. These solutions can be seen as "persistent", they are also sometimes called "bumps". We show that under very mild assumptions on the connectivity functions and because we do not use the Heaviside function for the nonlinearities, such solutions always exist. We also give sufficient conditions on the connectivity functions for the solution to be absolutely stable, that is to say independent of the initial state of the network. We then study the sensitivity of the solution(s) to variations of such parameters as the connectivity functions, the sigmoids, the external inputs, and, last but not least, the shape of the domain of existence Ω of the neural continuum networks. These theoretical results are illustrated and corroborated by a large number of numerical experiments in most of the cases $2 \leq n \leq 3$, $2 \leq q \leq 3$.

Key words: Neural masses, persistent states, integro-differential operators, compact operators, fixed points, stability, Lyapunov function

1 Introduction

We analyze the ability of neuronal continuum networks to display localized persistent activity or "bumps". This type of activity is related for example to working memory which involves the holding and processing of information on the time scale of seconds. Experiments in primates have shown that there exist neurons in the prefrontal cortex that have high firing rates during the period the animal is "remembering" the spatial location of an event before using the information being remembered [7], [19], [41]. Realistic models for this type of activity have involved spatially extended networks of coupled neural elements or neural masses and the study of spatially localized areas of high activity in these systems. A neuronal continuum network is first built from a "local" description of the dynamics of a number of interacting neuron populations where the spatial structure of the connections is neglected. This local description can be thought of as representing such a structure as a cortical column [42], [43], [5]. We call it a neural mass [18]. Probably the most well-known neural mass model is that of Jansen and Rit [32] based on the original work of Lopes Da Silva and colleagues [38],
[39] and of Van Rotterdam and colleagues
[52]. A complete analysis of the bifurcation diagram of this model can be found in [21]. The model has been used to simulate evoked potentials, i.e., EEG activities in normal [31] and epileptic patients [54], [53]. In a similar vein, David and Friston [10] have used an extension of this model to simulate a large variety of cerebral rhythms (α, β, γ, δ, and γ) in MEG/EEG simulations. Another important class of such models is the one introduced by Wilson and Cowan [56],
[30].

These local descriptions are then assembled spatially to form the neuronal continuum network. This continuum network is meant to represent a macroscopic part of the neocortex, e.g. a visual area such as V1. The spatial connections are models of cortico-cortical connections. Other, non-local connections with, e.g., such visual areas as the LGN or V2, are also considered. Other researchers have used several interconnected neural masses to simulate epileptogenic zones [54], [53], [37] or to study the connectivity between cortical areas [9]. In this paper we consider a continuum of neural masses.

2 The models

We briefly discuss local and spatial models.

* Corresponding author.
Email address: Olivier.Faugeras@sophia.inria.fr (Olivier Faugeras).

2.1 The local models

We consider n interacting populations of neurons such as those shown in figure 1. The figure is inspired by the work of Alex Thomson [50] and Wolfgang Maass [26]. It shows six populations of neurons. Red indicates excitation, blue inhibition. The thickness of the arrows pertain to the strength of the interaction. The six populations are located in layers 2/3, 4 and 5 of the neo-cortex.

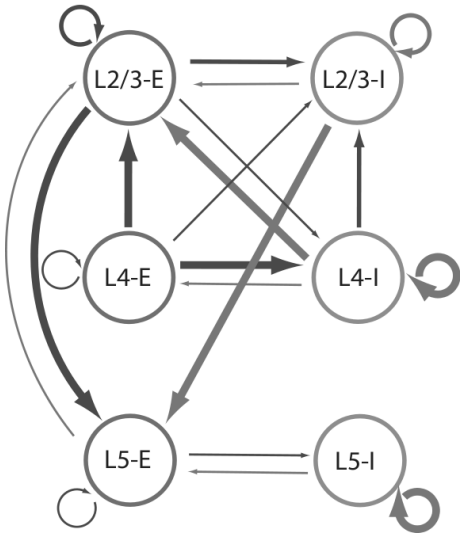

Fig. 1. A model with six interacting neural populations.

The following derivation follows closely that of Ermentrout [15]. We consider that each neural population i is described by its average membrane potential $V_i(t)$ or by its average instantaneous firing rate $\nu_i(t)$, the relation between the two quantities being of the form $\nu_i(t) = S_i(V_i(t))$ [20], [11], where S_i is sigmoidal and smooth. The functions S_i, $i = 1, \cdots, n$ satisfy the following properties introduced in the

Definition 2.1 *For all* $i = 1, \cdots, n$, $|S_i| \leq S_{im}$ *(boundedness). We note* $S_m = \max_i S_{im}$. *For all* $i = 1, \cdots, n$, *the derivative* S_i' *of* S_i *is positive and bounded by* $S_{im}' > 0$ *(boundedness of the derivatives). We note* $DS_m = \max_i S_{im}'$ *and* $D\mathbf{S}_m$ *the diagonal matrix* $diag(S_{im}')$.

A typical example of a function S_i is given in equation (15) below. Its shape is shown in figure 2 for the values of the parameters $\theta = 0$ and $s = 0.5,\ 1,\ 10$. We have $S_{im} = 1$ and $S_{im}' = s$. When $s \to \infty$, S converges to the Heaviside function H defined by

$$H(v) = \begin{cases} 0 & \text{if} \quad v < 0 \\ 1 & \text{otherwise} \end{cases}$$

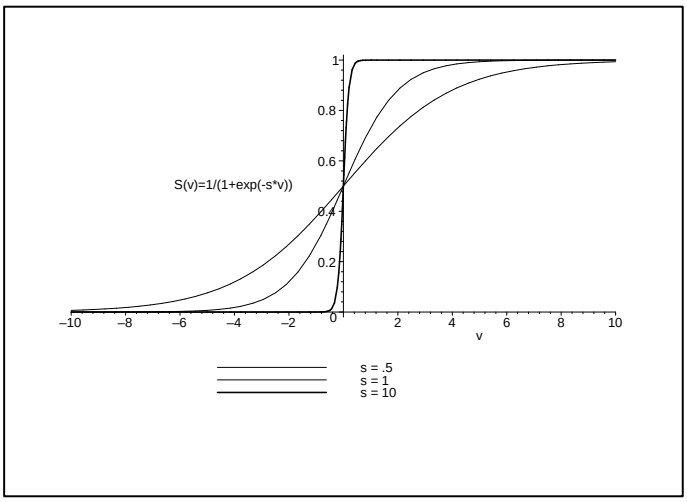

Fig. 2. Three examples of sigmoid functions for different values of the parameter s, see text.

Neurons in population j are connected to neurons in population i. A single action potential from neurons in population j is seen as a post-synaptic potential $PSP_{ij}(t-s)$ by neurons in population i, where s is the time of the spike hitting the terminal and t the time after the spike. We neglect the delays due to the distance travelled down the axon by the spikes.

Assuming that they sum linearly, the average membrane potential of population i due to action potentials of population j is

$$V_i(t) = \sum_k PSP_{ij}(t - t_k),$$

where the sum is taken over the arrival times of the spikes produced by the neurons in population j. The number of spikes arriving between t and $t + dt$ is $\nu_j(t)dt$. Therefore we have

$$V_i(t) = \sum_j \int_0^t PSP_{ij}(t-s)\nu_j(s)\, ds = \sum_j \int_0^t PSP_{ij}(t-s)S_j(V_j(s))\, ds,$$

or, equivalently

$$\nu_i(t) = S_i\left(\sum_j \int_0^t PSP_{ij}(t-s)\nu_j(s)\, ds\right) \tag{1}$$

The PSP_{ij} can depend on several variables in order to account for adaptation, learning, etc ...

There are two main simplifying assumptions that appear in the literature [15] and produce two different models.

2.1.1 The voltage-based model

The assumption, [29], is that the post-synaptic potential has the same shape no matter which presynaptic population caused it, the sign and amplitude may vary though. This leads to the relation

$$PSP_{ij}(t) = w_{ij} PSP_i(t).$$

If $w_{ij} > 0$ the population j excites population i whereas it inhibits it when $w_{ij} < 0$.

Finally, if we assume that $PSP_i(t) = A_i e^{-t/\tau_i} Y(t)$, or equivalently that

$$\tau_i \frac{dPSP_i(t)}{dt} + PSP_i(t) = A_i \delta(t), \tag{2}$$

we end up with the following system of ordinary differential equations

$$\tau_i \frac{dV_i(t)}{dt} + V_i(t) = \sum_j w_{ij} S_j(V_j(t)) + I^i_{\text{ext}}(t), \tag{3}$$

that describes the dynamic behaviour of a cortical column. We have incoporated the constant A_i in the weights w_{ij} and added an external current $I_{\text{ext}}(t)$ to model the non-local connections of population i. We introduce the $n \times n$ matrixes $\mathbf{W}$ such that $W_{ij} = w_{ij}/\tau_i$, and the function $\mathbf{S}$, $\mathbb{R}^n \to \mathbb{R}^n$ such that $\mathbf{S}(\mathbf{x})$ is the vector of coordinates $S_i(x_i)$, if $x = (x_1, \cdots, x_n)$. We rewrite (3) in vector form and obtain the following system of n ordinary differential equations

$$\dot{\mathbf{V}} = -\mathbf{L}\mathbf{V} + \mathbf{W}\,\mathbf{S}(\mathbf{V}) + \mathbf{I}_{\text{ext}}, \tag{4}$$

where $\mathbf{L}$ is the diagonal matrix $\mathbf{L} = \mathrm{diag}(1/\tau_{\mathrm{i}})$.

In terms of units, the left and righthand sides of this equations are in units of, say $\mathrm{mV} \times \mathrm{ms}^{-1}$. Therefore $\mathbf{I}_{\text{ext}}$, despite its name, is not a current. Note that since $\mathbf{S}(\mathbf{V})$ is an activity, its unit is ms^{-1} and hence $\mathbf{W}$ is in mV.

2.1.2 The activity-based model

The assumption is that the shape of a PSP depends only on the nature of the presynaptic cell, that is

$$PSP_{ij}(t) = w_{ij} PSP_j(t).$$

As above we suppose that $PSP_i(t)$ satisfies the differential equation (2) and define the time-averaged firing rate to be

$$A_j(t) = \int_0^t PSP_j(t-s)\nu_j(s)\,ds.$$

A similar derivation yields the following set of n ordinary differential equations

$$\tau_i \frac{dA_i(t)}{dt} + A_i(t) = S_i\left(\sum_j w_{ij}A_j(t) + I^i_{\text{ext}}(t)\right) i = 1, \cdots, n.$$

We include the τ_is in the sigmoids S_i and rewrite this in vector form

$$\dot{\mathbf{A}} = -\mathbf{L}\mathbf{A} + \mathbf{S}(\mathbf{W}\,\mathbf{A} + \mathbf{I}_{\text{ext}}), \tag{5}$$

The units are ms^{-2} for both sides of the equation. $\mathbf{W}$ is expressed in $\text{mV} \times \text{ms}$ and $\mathbf{I}_{\text{ext}}$ is in mV.

2.2 The continuum models

We now combine these local models to form a continuum of neural masses, e.g., in the case of a model of a significant part Ω of the cortex. We consider a subset Ω of $\mathbb{R}^q$, $q = 1, 2, 3$ which we assume to be connected and compact, i.e. closed and bounded. This encompasses several cases of interest.

When $q = 1$ we deal with one-dimensional sets of neural masses. Even though this appears to be of limited biological interest, this is one of the most widely studied cases because of its relative mathematical simplicity and because of the insights one can gain of the more realistic situations.

When $q = 2$ we discuss properties of two-dimensional sets of neural masses. This is perhaps more interesting from a biological point of view since Ω can be viewed as a piece of cortex where the third dimension, its thickness, is neglected. This case has received by far less attention than the previous one, probably because of the increased mathematical difficulty. Note that we could also take into account the curvature of the cortical sheet at the cost of an increase in the mathematical difficulty. This is outside the scope of this paper.

Finally $q = 3$ allows us to discuss properties of volumes of neural masses, e.g. cortical sheets where their thickness is taken into account [33], [6].

The theoretical results that are presented in this paper are independent of the value of q.

We note $\mathbf{V}(\mathbf{r}, t)$ (respectively $\mathbf{A}(\mathbf{r}, t)$) the n-dimensional state vector at the point $\mathbf{r}$ of the continuum and at time t. We introduce the $n \times n$ matrix function $\mathbf{W}(\mathbf{r},\, \mathbf{r}')$

which describes how the neural mass at point $\mathbf{r}'$ influences that at point $\mathbf{r}$ at time t. We call $\mathbf{W}$ the connectivity matrix function. In particular, $\mathbf{W}(\mathbf{r}, \mathbf{r}) = \mathbf{W}$, the matrix that appears in equations (4) and (5). More precisely, $W_{ij}(\mathbf{r}, \mathbf{r}')$ describes how population j at point $\mathbf{r}'$ influences population i at point $\mathbf{r}$ at time t. Equation (4) can now be extended to

$$\mathbf{V}_t(\mathbf{r}, t) = -\mathbf{L}\mathbf{V}(\mathbf{r}, t) + \int_\Omega \mathbf{W}(\mathbf{r}, \mathbf{r}')\mathbf{S}(\mathbf{V}(\mathbf{r}', t))\, d\mathbf{r}' + \mathbf{I}_{\text{ext}}(\mathbf{r}, t), \tag{6}$$

and equation (5) to

$$\mathbf{A}_t(\mathbf{r}, t) = -\mathbf{L}\mathbf{A}(\mathbf{r}, t) + \mathbf{S}\left(\int_\Omega \mathbf{W}(\mathbf{r}, \mathbf{r}')\mathbf{A}(\mathbf{r}', t))\, d\mathbf{r}' + \mathbf{I}_{\text{ext}}(\mathbf{r}, t)\right). \tag{7}$$

It is important to discuss again the units of the quantities involved in these equations. For equation (6), as for equation (3) the unit is $\mathrm{mV} \times \mathrm{ms}^{-1}$ for both sides. Because of the spatial integration, $\mathbf{W}$ is in $\mathrm{mV} \times \mathrm{ms}^{-1} \times \mathrm{mm}^{-q}$, q is the dimension of the continuum. To obtain a dimensionless equation we normalize, i.e. divide both sides of the equation, by the Frobenius norm $\|\mathbf{W}\|_F$ of the connectivity matrix function $\mathbf{W}$ (see appendix A.1 for a definition). Equivalently, we assume that $\|\mathbf{W}\|_F = 1$.

We have given elsewhere [**?**], but see proposition 3.2 below for completeness, sufficient conditions on $\mathbf{W}$ and $\mathbf{I}_{\text{ext}}$ for equations (6) and (7) to be well-defined and studied the existence and stability of their solutions for general and homogeneous (i.e. independent of the space variable) external currents. In this article we analyze in detail the case of stationary external currents, i.e. independent of the time variable, and investigate the existence and stability of the corresponding stationary solutions of (6) and (7).

A significant amount of work has been devoted to this or closely related problems, starting perhaps with the pioneering work of Wilson and Cowan
[56]. A fairly recent review of this work, and much more, can be found in a paper by Coombes [8]. Amari [1] investigated the problem in the case $n = q = 1$ when the sigmoid function is approximated by a Heaviside function and the connectivity function has a "Mexican-hat shape". He proved the existence of stable bumps in this case. His work has been extended to different firing-rate and connectivity functions
[24], [35], [36], [47],
[23], [22].

The case $n = 1$, $q = 2$ has been considered by several authors including
[44], [45] for general firing-rate functions and Gaussian-like connectivity functions, and [3] when the firing-rate functions are approximated by Heaviside functions.

Extending these analysis to two- or three-dimensional continuum is difficult because of the increase in the degrees of freedom in the choice of the connectivity function. The case $n = 2$, $q = 1$ has been studied in [55], [4] when the firing-rate

functions are approximated by Heaviside functions and the connectivity function is circularly symmetric while the case $n = 2$, $q = 2$ is mentioned as difficult in [14].

In all these contributions, the proof of the existence of a bump solution is based upon the original Amari's argument [1] which works only when $q = 1$ and the firing rate function is approximated by a Heaviside function. Solutions are usually constructed using a variant of the method of the singular perturbation construction, e.g., [45] which is usually fairly heavy. Sufficient conditions for their stability are obtained by a linear stability analysis which in general requires the use of Heaviside functions instead of sigmoids.

The approach that we describe in this paper is a significant departure from the previous ones. By using simple ideas of functional analysis we are able to

(1) Prove the existence and uniqueness of a stationary solution to equations (6) and (7) for any dimensions n and q, arbitrary connectivity functions and general firing-rate functions.
(2) Obtain very simple conditions for the absolute stability of the solution in terms of the spectrum of the differential of the nonlinear operator that appears in the righthand side of equations (6) and (7).
(3) Construct a numerical approximation as accurate as needed of the solution, when it exists, for any stationary input.
(4) Characterize the sensitivity of the solutions to variations of the parameters, including the shape of the domain Ω.

To be complete, let us point out that equations of the type of (6) and (7) have been studied in pure mathematics, see e.g.[28]. They are of the Hammerstein type [27,51]. This type of equations has received some recent attention, see [2], and progress have been made toward a better understanding of their solutions. Our contributions are the articulation of the models of networks of neural masses with this type of equation, the characterization of persistent activity in these networks as fixed points of Hammerstein equations, the proof of the existence of solutions, the characterization of their stability and the analysis of their sensitivity to variations of the parameters involved in the equations.

3 Existence of stationary solutions

In this section we deal with the problem of the existence of stationary solutions to (6) and (7) for a given stationary external current $\mathbf{I}_{\rm ext}$.

As indicated in the previous section, we use functional analysis to solve this problem. Let $\mathcal{F}$ be the set $\mathbf{L}^2_n(\Omega)$ of square integrable functions from Ω to $\mathbb{R}^n$. This is a

Hilbert, hence a Banach, space for the usual inner product

$$\langle \mathbf{V}_1,\, \mathbf{V}_2 \rangle = \int_\Omega \mathbf{V}_1(\mathbf{r})^T \overline{\mathbf{V}_2}(\mathbf{r})\, d\mathbf{r},$$

where $\overline{\mathbf{V}}$ is the complex conjuguate of the vector $\mathbf{V}$. This inner product induces the norm $\|\mathbf{V}\|^2_{\mathcal{F}} = \sum_{i=1,\cdots,n} \int_\Omega |V_i(\mathbf{r})|^2\, d\mathbf{r}$, see appendix A.1. $\mathcal{F}$ is the state space. Another important space is $\mathbf{L}^2_{n\times n}(\Omega\times\Omega))$, the space of "square integrable $n\times n$ matrices", see appendix A.1 for a precise definition. We assume that the connectivity matrix functions $\mathbf{W}(\cdot,\cdot)$ are in this space, see propositions 3.1 and 3.2 below.

We also identify $\mathbf{L}^2_{n\times n}(\Omega\times\Omega))$ with $\mathcal{L}\,(\mathcal{F})$ (the space of continuous linear operators on $\mathcal{F}$) as follows. If $\mathbf{W} \in \mathbf{L}^2_{n\times n}(\Omega\times\Omega))$ it defines a linear mapping

$$\begin{aligned} \mathbf{W} : \mathcal{F} &\longrightarrow \mathcal{F} \quad \text{such that} \\ \mathbf{X} \to \mathbf{W}\cdot\mathbf{X} &= \textstyle\int_\Omega \mathbf{W}(.,\mathbf{r}')\mathbf{X}(\mathbf{r}')d\mathbf{r}' \end{aligned}$$

For example this allows us to write (6) and (7)

$$\begin{aligned} \mathbf{V}_t &= -\mathbf{L}\mathbf{V} + \mathbf{W}\cdot\mathbf{S}\,(\mathbf{V}) + \mathbf{I}_{\text{ext}} \\ \mathbf{A}_t &= -\mathbf{L}\mathbf{A} + \mathbf{S}(\mathbf{W}\cdot\mathbf{A} + \mathbf{I}_{\text{ext}}) \end{aligned}$$

We first recall some results on the existence of a solution to (6) and (7) that will be used in the sequel.

We denote by J a closed interval of the real line containing 0. A state vector $\mathbf{X}(\mathbf{r},t)$ is a mapping $\mathbf{X} : \mathrm{J} \to \mathcal{F}$ and equations (6) and (7) are formally recast as an initial value problem:

$$\begin{cases} \mathbf{X}'(t) = f(t,\mathbf{X}(t)) \\ \mathbf{X}(0) = \mathbf{X}_0 \end{cases} \tag{8}$$

where $\mathbf{X}_0$ is an element of $\mathcal{F}$ and the function f from $\mathrm{J}\times\mathcal{F}$ is defined by the righthand side of (6), in which case we call it f_v, or (7), in which case we call it f_a. In other words, equations (6) and (7) become differential equations defined on the Hilbert space $\mathcal{F}$.

We need the following two propositions that we quote without proof [**?**].

Proposition 3.1 *If the following two hypotheses are satisfied.*

(1) The connectivity function $\mathbf{W}$ *is in* $\mathbf{L}^2_{n\times n}(\Omega\times\Omega))$ *(see appendix A.1),*
(2) At each time instant $t \in \mathrm{J}$ *the external current* $\mathbf{I}$ *is in* $C(\mathrm{J};\mathcal{F})$*, the set of continuous functions from* J *to* $\mathcal{F}$*,*

then the mappings f_v and f_a are from $\mathrm{J} \times \mathcal{F}$ to $\mathcal{F}$, continuous, and Lipschitz continuous with respect to their second argument, uniformly with respect to the first.

Proposition 3.2 *If the following two hypotheses are satisfied*

(1) The connectivity function $\mathbf{W}$ is in $\mathbf{L}^2_{n\times n}(\Omega \times \Omega)$),
(2) the external current $\mathbf{I}_{\mathrm{ext}}$ is in $C(\mathrm{J}; \mathcal{F})$, the set of continuous functions from J to $\mathcal{F}$,

then for any function $\mathbf{X}_0$ in $\mathcal{F}$ there is a unique solution $\mathbf{X}$, defined on $\mathbb{R}$ (and not only on J) and continuously differentiable, of the abstract initial value problem (8) for $f = f_v$ and $f = f_a$.

This proposition says that, given the two hypotheses and the initial condition, there exists a unique solution to (6) or (7) and that this solution is in $C^1(\mathbb{R}; \mathcal{F})$, the set of continuously differentiable functions from $\mathbb{R}$ to $\mathcal{F}$.

We now turn our attention to a special type of solutions of (6) and (7), corresponding to stationary external currents. We call these solutions, when they exist, stationary solutions. The currents $\mathbf{I}_{\mathrm{ext}}$ are simply in $\mathcal{F}$.

A stationary solution of (6) or (7) is defined by

$$\mathbf{X} = f^L(\mathbf{X}), \tag{9}$$

where the function f^L, $\mathcal{F} \to \mathcal{F}$, is equal to f^L_v defined by

$$f^L_v(\mathbf{V})(\mathbf{r}) = \int_\Omega \mathbf{W}^L(\mathbf{r}, \mathbf{r}')\mathbf{S}(\mathbf{V}(\mathbf{r}'))\, d\mathbf{r}' + \mathbf{I}^L_{\mathrm{ext}}(\mathbf{r}), \tag{10}$$

or to f^L_a defined by

$$f^L_a(\mathbf{A})(\mathbf{r}) = \mathbf{S}^L \left(\int_\Omega \mathbf{W}(\mathbf{r}, \mathbf{r}')\mathbf{A}(\mathbf{r}')\, d\mathbf{r}' + \mathbf{I}_{\mathrm{ext}}(\mathbf{r}) \right), \tag{11}$$

where $\mathbf{W}^L = \mathbf{L}^{-1}\mathbf{W}$, $\mathbf{S}^L = \mathbf{L}^{-1}\mathbf{S}$ and $\mathbf{I}^L_{\mathrm{ext}} = \mathbf{L}^{-1}\mathbf{I}_{\mathrm{ext}}$.

We now recall the

Definition 3.3 *A continuous mapping $M : \mathcal{F} \to \mathcal{F}$ (linear or nonlinear) is called compact provided that for each bounded subset $\mathcal{B}$ of $\mathcal{F}$, the set $M(\mathcal{B})$ is relatively compact, i.e. its closure is compact.*

We then consider the nonlinear mapping $g^L_v : \mathcal{F} \to \mathcal{F}$

$$g^L_v(\mathbf{V})(\mathbf{r}) = \int_\Omega \mathbf{W}^L(\mathbf{r}, \mathbf{r}')\mathbf{S}(\mathbf{V}(\mathbf{r}'))\, d\mathbf{r}' \tag{12}$$

and the linear mappings g_a and g_a^L

$$g_a(\mathbf{A})(\mathbf{r}) = \int_\Omega \mathbf{W}(\mathbf{r},\mathbf{r}')\mathbf{A}(\mathbf{r}')\,d\mathbf{r}', \tag{13}$$

$$g_a^L(\mathbf{A})(\mathbf{r}) = \int_\Omega \mathbf{W}^L(\mathbf{r},\mathbf{r}')\mathbf{A}(\mathbf{r}')\,d\mathbf{r}'. \tag{14}$$

We have the following

Proposition 3.4 *If* $\mathbf{W} \in \mathbf{L}^2_{n\times n}(\Omega\times\Omega)$, g_v^L *and* g_a^L *are compact operators of* $\mathcal{F}$.

Proof. We know from proposition 3.1 that g_v^L is continuous and prove that for each sequence $\{\mathbf{V}_n\}_{n=1}^\infty$ of $\mathcal{F}$ there exists a subsequence $\{\mathbf{V}_{n_j}\}_{j=1}^\infty$ such that $g_v^L(\mathbf{V}_{n_j})$ is convergent in $\mathcal{F}$.

Because of the definition 2.1 of $\mathbf{S}$ the sequence $\{\mathbf{A}_n = \mathbf{S}(\mathbf{V}_n)\}_{n=1}^\infty$ is bounded in $\mathcal{F}$ by $C = S_m\sqrt{n|\Omega|} > 0$. We prove that there exists a subsequence $\{\mathbf{A}_{n_j}\}_{j=1}^\infty$ such that $\{g_a^L(\mathbf{A}_{n_j}) = g_v^L(\mathbf{V}_{n_j})\}_{j=1}^\infty$ converges in $\mathcal{F}$.

Since Since $\mathcal{F}$ is separable, its unit ball is weakly compact and because $\{\mathbf{A}_n\}_{n=1}^\infty$ is bounded there exists a a subsequence $\{\mathbf{A}_{n_j}\}_{j=1}^\infty$ of $\{\mathbf{A}_n\}_{n=1}^\infty$ that converges weakly in $\mathcal{F}$ toward $\mathbf{A}$. Because of Fubini's theorem, for almost all $\mathbf{r}\in\Omega$ (noted a.s.) the function $\mathbf{r}' \to \mathbf{W}(\mathbf{r},\mathbf{r}')$ is in $\mathcal{F}$. Therefore, a.s., $\mathbf{B}_{n_j} = g_a^L(\mathbf{A}_{n_j}) \to \mathbf{B}$.

Since $\|\mathbf{A}\|_\mathcal{F} \le \liminf_{j\to\infty}\|\mathbf{A}_{n_j}\|_\mathcal{F} \le C$, $\mathbf{A}$ is also bounded by C in $\mathcal{F}$. It is easy to show that $\|\mathbf{B}_{n_j}-\mathbf{B}\|^2_\mathcal{F} \le 2C\|\mathbf{W}\|_F$ and we can apply Lebesgue's Dominated Convergence Theorem to the sequence $\mathbf{B}_{n_j}(\mathbf{r}) - \mathbf{B}(\mathbf{r})$ and conclude that $\|\mathbf{B}_{n_j} - \mathbf{B}\|_\mathcal{F} \to 0$, i.e., $g_v^L(\mathbf{V}_{n_j})$ is convergent in $\mathcal{F}$.

A small variation of the proof shows that g_a^L is compact. □

From proposition 3.4 follows the

Proposition 3.5 *Under the hypotheses of proposition 3.4, if* $\mathbf{I}_{\text{ext}} \in \mathcal{F}$, f_v^L *and* f_a^L, *are compact operators of* $\mathcal{F}$.

Proof. The operators $\mathbf{X} \to \mathbf{I}^L_{\text{ext}}$ and $\mathbf{X} \to \mathbf{I}_{\text{ext}}$ are clearly compact under the hypothesis $\mathbf{I}_{\text{ext}} \in \mathcal{F}$, therefore f_v^L is the sum of two compact operators, hence compact. For the same reason $g_a + \mathbf{I}_{\text{ext}}$ is also compact and so is $f_a^L = \mathbf{S}^L(g_a + \mathbf{I}_{\text{ext}})$ because $\mathbf{S}^L$ is smooth and bounded. □

We can now prove the

Theorem 3.6 *If* $\mathbf{W} \in \mathbf{L}^2_{n\times n}(\Omega\times\Omega)$ *and* $\mathbf{I}_{\text{ext}} \in \mathcal{F}$, *there exists a stationary solution of (6) and (7).*

Proof. A stationary solution of (6) (respectively of (7)) is a fixed point of f_v^L (respectively of f_a^L).

Define the set $\mathcal{C}_v = \{\mathbf{V} \in \mathcal{F} | \mathbf{V} = \lambda f_v^L(\mathbf{V}) \quad \text{for some} \quad 0 \leq \lambda \leq 1\}$. Because of lemma A.2 for all $\mathbf{V} \in \mathcal{C}_v$ we have

$$\|\mathbf{V}\|_{\mathcal{F}} \leq \lambda(\|g_v^L(\mathbf{V})\|_{\mathcal{F}} + \|\mathbf{I}_{\text{ext}}^L\|_{\mathcal{F}}) \leq \lambda(S_m\sqrt{n|\Omega|}\|\mathbf{W}^L\|_F + \|\mathbf{I}_{\text{ext}}^L\|_{\mathcal{F}}),$$

hence $\mathcal{C}_v$ is bounded.

Similarly define the set $\mathcal{C}_a = \{\mathbf{A} \in \mathcal{F} | \mathbf{A} = \lambda f_a^L(\mathbf{A}) \quad \text{for some} \quad 0 \leq \lambda \leq 1\}$. Because of lemma A.2 for all $\mathbf{A} \in \mathcal{C}_a$ we have $\|\mathbf{A}\|_{\mathcal{F}} \leq \lambda S_m\sqrt{n|\Omega|}$, hence $\mathcal{C}_a$ is bounded.

The conclusion follows from Schaefer's fixed point theorem [16]. □

4 Stability of the stationary solutions

In this section we give a sufficient condition on the connectivity matrix $\mathbf{W}$ to guarantee the stability of the stationary solutions to (6) and (7).

4.1 The voltage-based model

We define the "corrected maximal" connectivity function $\mathbf{W}_{cm}(\mathbf{r}, \mathbf{r}')$ by $\mathbf{W}_{cm} = \mathbf{W}D\mathbf{S}_m$, where $D\mathbf{S}_m$ is defined in definition 2.1. We also define the corresponding linear operator $h_m : \mathcal{F} \to \mathcal{F}$

$$h_m(\mathbf{V})(\mathbf{r}) = \int_\Omega \mathbf{W}_{cm}(\mathbf{r}, \mathbf{r}')\mathbf{V}(\mathbf{r}')\, d\mathbf{r}'$$

which is compact according to proposition 3.4. Its adjoint, noted h_m^* is defined [1] by

$$h_m^*(\mathbf{V})(\mathbf{r}) = \int_\Omega \mathbf{W}_{cm}^T(\mathbf{r}', \mathbf{r})\mathbf{V}(\mathbf{r}')\, d\mathbf{r}',$$

and is also compact. Hence the symmetric part $h_m^s = \frac{1}{2}(h_m + h_m^*)$, the sum of two compact operators, is also compact. Furthermore we have $\langle \mathbf{V}, h_m(\mathbf{V})\rangle = \langle \mathbf{V}, h_m^s(\mathbf{V})\rangle$, as can be easily verified. It is also self-adjoint since, clearly, $h_m^s = h_m^{s*}$.

We recall the following property of the spectrum of a compact self-adjoint operator in a Hilbert space (see, e.g., [13]).

Proposition 4.1 *The spectrum of a compact, self-adjoint operator of a Hilbert space is countable and real. Each nonzero spectral value is an eigenvalue and the dimension of the corresponding eigenspace is finite.*

[1] By definition, $\langle \mathbf{V}_1,\ h_m(\mathbf{V}_2)\rangle = \langle h_m^*(\mathbf{V}_1), \mathbf{V}_2\rangle$, for all elements $\mathbf{V}_1$, $\mathbf{V}_2$ of $\mathcal{F}$.

We have the following

Theorem 4.2 *A sufficient condition for the stability of a stationary solution to (6) is that all the eigenvalues of the linear compact, self-adjoint, operator $h_m^{L,\,s}$ be less than 1, where $h_m^{L,\,s}$ is defined by*

$$h_m^{L,\,s}(\mathbf{x})(\mathbf{r}) = \frac{1}{2}\int_\Omega \mathbf{L}^{-1/2}(\mathbf{W}_{cm}^T(\mathbf{r}',\mathbf{r}) + \mathbf{W}_{cm}(\mathbf{r},\mathbf{r}'))\mathbf{L}^{-1/2}\,\mathbf{x}(\mathbf{r}')\,d\mathbf{r}'\,\forall \mathbf{x}\in\mathcal{F},$$

where $h_m^{L,\,s}$ is the symmetric part of the linear compact operator $h_m^L : \mathcal{F}\to\mathcal{F}$:

$$h_m^L(\mathbf{x})(\mathbf{r}) = \int_\Omega \mathbf{L}^{-1/2}\mathbf{W}_{cm}(\mathbf{r},\mathbf{r}')\mathbf{L}^{-1/2}\,\mathbf{x}(\mathbf{r}')\,d\mathbf{r}'$$

Proof. The proof of this theorem is a generalization to the continuum case of a result obtained by Matsuoka [40].

Let us note $\underline{\mathbf{S}}$ the function $(D\mathbf{S}_m)^{-1}\mathbf{S}$ and rewrite equation (6) for an homogeneous input $\mathbf{I}_{ext}$ as follows

$$\mathbf{V}_t(\mathbf{r},t) = -\mathbf{L}\mathbf{V}(\mathbf{r},t) + \int_\Omega \mathbf{W}_{cm}(\mathbf{r},\mathbf{r}')\underline{\mathbf{S}}(\mathbf{V}(\mathbf{r}',t)\,d\mathbf{r}' + \mathbf{I}_{ext}(\mathbf{r}).$$

Let $\mathbf{U}$ be a stationary solution of (6). Let also $\mathbf{V}$ be the unique solution of the same equation with initial some condition $\mathbf{V}(0) = \mathbf{V}_0 \in \mathcal{F}$, see proposition 3.2. We introduce the new function $\mathbf{X} = \mathbf{V} - \mathbf{U}$ which satisfies

$$\mathbf{X}_t(\mathbf{r},t) = -\mathbf{L}\mathbf{X}(\mathbf{r},t) + \int_\Omega \mathbf{W}_{cm}(\mathbf{r},\mathbf{r}')\mathbf{\Theta}(\mathbf{X}(\mathbf{r}',t))\,d\mathbf{r}' = -\mathbf{L}\mathbf{X}(\mathbf{r},t) + h_m(\mathbf{\Theta}(\mathbf{X}))(\mathbf{r},t)$$

where the vector $\mathbf{\Theta}(\mathbf{X})$ is given by $\mathbf{\Theta}(\mathbf{X}(\mathbf{r},t)) = \underline{\mathbf{S}}(\mathbf{V}(\mathbf{r},t)) - \underline{\mathbf{S}}(\mathbf{U}(\mathbf{r})) = \underline{\mathbf{S}}(\mathbf{X}(\mathbf{r},t) + \mathbf{U}(\mathbf{r})) - \underline{\mathbf{S}}(\mathbf{U}(\mathbf{r}))$. Consider now the functional

$$\Delta(\mathbf{X}) = \int_\Omega \left(\sum_{i=1}^n \int_0^{X_i(\mathbf{r},t)} \Theta_i(z)\,dz\right)\,d\mathbf{r}.$$

We note that

$$z \le \Theta_i(z) < 0 \quad \text{for} \quad z<0 \quad \text{and} \quad 0 < \Theta_i(z) \le z \quad \text{for} \quad z>0,\ \Theta_i(0)=0,\ i=1,\cdots,n.$$

This is because (Taylor expansion with integral remainder):

$$\Theta_i(z) = \underline{S}_i(z+U_i) - \underline{S}_i(U_i) = z\int_0^1 \underline{S}_i'(U_i+\zeta z)\,d\zeta,$$

and $0 < \underline{S}_i' \le 1$ by construction of the vector $\underline{\mathbf{S}}$. This implies that the functional $\Delta(\mathbf{X})$ is strictly positive for all $\mathbf{X}\in\mathcal{F}\neq 0$ and $\Delta(0)=0$. It also implies, and this is used in the sequel, that $z\Theta_i(z) \ge \Theta_i(z)^2$.

The time derivative of Δ is readily obtained:

$$\frac{d\Delta(\mathbf{X})}{dt} = \int_\Omega \mathbf{\Theta}^T(\mathbf{X}(\mathbf{r},t))\mathbf{X}_t(\mathbf{r},t))\,d\mathbf{r} = \langle\, \mathbf{\Theta}(\mathbf{X}),\, \mathbf{X}_t \,\rangle$$

We replace $\mathbf{X}_t(\mathbf{r},t))$ by its value in this expression to obtain

$$\frac{d\Delta(\mathbf{X})}{dt} = -\langle\, \mathbf{\Theta}(\mathbf{X}),\, \mathbf{L}\mathbf{X} \,\rangle + \langle\, \mathbf{\Theta}(\mathbf{X}),\, h_m(\mathbf{\Theta}(\mathbf{X})) \,\rangle$$

Because of a previous remark we have

$$\mathbf{X}^T(\mathbf{r},t))\mathbf{L}\mathbf{\Theta}(\mathbf{X}(\mathbf{r},t)) \geq \mathbf{\Theta}^T(\mathbf{X}(\mathbf{r},t))\mathbf{L}\mathbf{\Theta}(\mathbf{X}(\mathbf{r},t)),$$

and this provides up with an upper bound for $\frac{d\Delta(\mathbf{X})}{dt}$:

$$\frac{d\Delta(\mathbf{X})}{dt} \leq \langle\, \mathbf{\Theta}(\mathbf{X}),\, (-\mathbf{L} + h_m^s).\mathbf{\Theta}(\mathbf{X}) \,\rangle = \left\langle\, \mathbf{L}^{1/2}\mathbf{\Theta}(\mathbf{X}),\, (-\mathrm{Id} + h_m^{L,s})\,\mathbf{L}^{1/2}\mathbf{\Theta}(\mathbf{X}) \,\right\rangle,$$

and the conclusion follows. □

Note that we have the following

Corollary 4.3 *If the condition of theorem 4.2 is satisfied, the homogeneous solution of (6) is unique.*

Proof. Indeed, the result of theorem 4.2 is independent of the particular stationary solution $\mathbf{U}$ that is chosen in the proof. □

4.2 The activity-based model

We now give a sufficient condition for the stability of a solution to (7). We define the "maximal corrected" connectivity matrix function $\mathbf{W}_{mc} = D\mathbf{S}_m\mathbf{W}$ and the linear compact operator k_m from $\mathcal{F}$ to $\mathcal{F}$

$$k_m(\mathbf{x})(\mathbf{r}) = \int_\Omega \mathbf{W}_{mc}(\mathbf{r},\mathbf{r}')\,\mathbf{x}(\mathbf{r}')\,d\mathbf{r}'.$$

Theorem 4.4 *A sufficient condition for the stability of a solution to (7) is that all the eigenvalues of the linear compact operator k_m^L be of magnitude less than 1, where k_m^L is defined by*

$$k_m^L(\mathbf{x})(\mathbf{r}) = \int_\Omega \mathbf{L}^{-1/2}\mathbf{W}_{mc}(\mathbf{r},\mathbf{r}')\mathbf{L}^{-1/2}\mathbf{x}(\mathbf{r}')\,d\mathbf{r}' \quad \forall \mathbf{x} \in \mathcal{F}$$

Proof. Let $\mathbf{U}$ be a stationary solution of (7) for a stationary external current $\mathbf{I}_{\mathrm{ext}}(\mathbf{r})$. As in the proof of theorem 4.2 we introduce the new function $\mathbf{X} = \mathbf{V} - \mathbf{U}$, where $\mathbf{V}$

is the unique solution of the same equation with initial conditions $\mathbf{V}(0) = \mathbf{V}_0 \in \mathcal{F}$, an element of $C(J, \mathcal{F})$. We have

$$\mathbf{X}_t(\mathbf{r}, t) = -\mathbf{L}\mathbf{X}(\mathbf{r}, t) + \mathbf{S}\left(\int_\Omega \mathbf{W}(\mathbf{r}, \mathbf{r}')\mathbf{V}(\mathbf{r}', t)\, d\mathbf{r}' + \mathbf{I}_{\text{ext}}(\mathbf{r})\right) - \mathbf{S}\left(\int_\Omega \mathbf{W}(\mathbf{r}, \mathbf{r}')\mathbf{U}(\mathbf{r}')\, d\mathbf{r}' + \mathbf{I}_{\text{ext}}(\mathbf{r})\right)$$

Using a first-order Taylor expansion with integral remainder this equation can be rewritten as

$$\mathbf{X}_t(\mathbf{r}, t) = -\mathbf{L}\mathbf{X}(\mathbf{r}, t) + \left(\int_0^1 D\mathbf{S}\Big(\int_\Omega \mathbf{W}(\mathbf{r}, \mathbf{r}')\mathbf{U}(\mathbf{r}')\, d\mathbf{r}' + \mathbf{I}_{\text{ext}}(\mathbf{r}) + \zeta \int_\Omega \mathbf{W}(\mathbf{r}, \mathbf{r}')\mathbf{X}(\mathbf{r}', t)\, d\mathbf{r}'\Big)\, d\zeta\right) \left(\int_\Omega \mathbf{W}(\mathbf{r}, \mathbf{r}')\mathbf{X}(\mathbf{r}', t)\, d\mathbf{r}'\right)$$

Consider now the functional $\Delta(\mathbf{X}) = \frac{1}{2}\|\mathbf{X}\|^2_{\mathcal{F}}$. Its time derivative is:

$$\frac{d\Delta(\mathbf{X})}{dt} = \langle\, \mathbf{X},\, \mathbf{X}_t \,\rangle$$

We replace $\mathbf{X}_t(\mathbf{r}, t))$ by its value in this expression to obtain

$$\frac{d\Delta(\mathbf{X})}{dt} = -\langle\, \mathbf{X},\, \mathbf{L}\mathbf{X} \,\rangle + \langle\, \mathbf{X},\, \sigma_m(\mathbf{X})k_m(\mathbf{X}) \,\rangle\,,$$

where the nonlinear operator σ_m is defined by

$$\sigma_m(\mathbf{X})(\mathbf{r}, t) = \int_0^1 D\mathbf{S}\Big(\int_\Omega \mathbf{W}(\mathbf{r}, \mathbf{r}')\mathbf{U}(\mathbf{r})\, d\mathbf{r}' + \zeta \int_\Omega \mathbf{W}(\mathbf{r}, \mathbf{r}')\mathbf{X}(\mathbf{r}', t)\, d\mathbf{r}'\Big)\, D\mathbf{S}_m^{-1}\, d\zeta,$$

a diagonal matrix whose diagonal elements are between 0 and 1. We rewrite $\frac{d\Delta(\mathbf{X})}{dt}$ in a slightly different manner, introducing the operator k_m^L

$$\frac{d\Delta(\mathbf{X})}{dt} = -\left\langle\, \mathbf{L}^{1/2}\mathbf{X},\, \mathbf{L}^{1/2}\mathbf{X} \,\right\rangle + \left\langle\, \sigma_m(\mathbf{X})\mathbf{L}^{1/2}\mathbf{X},\, k_m^L(\mathbf{L}^{1/2}\mathbf{X}) \,\right\rangle,$$

From the Cauchy-Schwarz' inequality and the property of $\sigma_m(\mathbf{X})$ we obtain

$$\left|\left\langle\, \sigma_m(\mathbf{X})\mathbf{Y},\, k_m^L(\mathbf{Y}) \,\right\rangle\right| \leq \|\sigma_m(\mathbf{X})\mathbf{Y}\|_{\mathcal{F}}\, \|k_m^L(\mathbf{Y})\|_{\mathcal{F}} \leq \|\mathbf{Y}\|_{\mathcal{F}}\, \|k_m^L(\mathbf{Y})\|_{\mathcal{F}} \quad \mathbf{Y} = \mathbf{L}^{1/2}\mathbf{X}$$

A sufficient condition for $\frac{d\Delta(\mathbf{X})}{dt}$ to be negative is therefore that $\|k_m^L(\mathbf{Y})\|_{\mathcal{F}} < \|\mathbf{Y}\|_{\mathcal{F}}$ for all $\mathbf{Y}$. □

5 Numerical experiments

In this section and the next we investigate the question of effectively, i.e. numerically, computing stationary solutions of (6) which is equivalent to computing solutions of (9). Similar results are obtained for (7).

In all our numerical experiments, we assume the sigmoidal functions $S_i,\ i = 1, \cdots, n$ introduced in the definition 2.1 to be of the form

$$S_i(v) = \frac{1}{1 + e^{-s_i(v-\theta_i)}}. \tag{15}$$

This function is symmetric with respect to the "threshold" potential θ_i, see section 6.1.3, and varies between 0 and 1. The positive parameter s_i controls the slope of the ith sigmoid at $v = \theta_i$, see section 6.1.4 and figure 2.

5.1 Algorithm

We now explain how to compute a fixed point $\mathbf{V}^f$ of equation (10) in which we drop for simplicity the upper index L and the lower index ext:

$$\mathbf{V}^f = \mathbf{W} \cdot \mathbf{S}(\mathbf{V}^f) + \mathbf{I} \tag{16}$$

The method is iterative and based on Banach's fixed point theorem [16]:

Theorem 5.1 *Let X be Banach space and $M : X \to X$ a nonlinear mapping such that*

$$\forall x, y \in X,\ \|M(x) - M(y)\| \leq q \|x - y\|,\ \ 0 < q < 1$$

Such a mapping is said contracting. M has a unique fixed point x^f and for all $x_0 \in X$ and $x_{p+1} = M(x_p)$ then (x_p) converges geometrically to x^f.

Note that this method only allows to compute the solution of (9) when it admits a unique solution and f is contracting. However it could admit more than one solution (recall it always has a solution, see theorem 3.6) or f could be non-contracting. Another method has to be found in these cases.

In our case : $X = \mathcal{F} = \mathbf{L}^2_n(\Omega)$ where Ω is an open bounded set of $\mathbb{R}^n$ and $M = f_v$. According to lemmas A.2 and A.1, if $DS_m\ \|\mathbf{W}\|_F < 1$, f_v is contracting.

Each element of the sequence $\mathbf{V}_p,\ p \geq 0$ is approximated by a piecewise constant function $\mathbf{V}_{p,h}$, where h is the step of the approximation, defined by a finite number of points $\mathbf{r}_{h,j} \in \Omega,\ 1 \leq j \leq \lfloor \frac{1}{h} \rfloor$. In order to avoid difficulties because $\mathbf{V}_{p,h} \in \mathbf{L}^2_n(\Omega)$, hence defined almost everywhere, we assume that $\mathbf{W}$ and $\mathbf{I}$ are smooth. It is not a restriction because every function of $\mathbf{L}^2_n(\Omega)$ can be approximated by a

smooth function. As the bump solution is smooth as soon as $\mathbf{W}, \mathbf{I}$ are smooth, we can use the multidimensional Gaussian quadrature formula [46], [49] with N points (in the examples below, usually $N = 20$) on each axis. In order to interpolate the values of the bump from a finite (and small) number of its values $\mathbf{V}_n(\mathbf{r}_{h,j,Gauss})$, we use Nyström's method [28, Section: Fredholm equation, numerical methods] stated as follows:

$$\mathbf{V}_p(\mathbf{r}) = \sum_j g_j \mathbf{W}_p(\mathbf{r},\, \mathbf{r}_{p,j,Gauss}) \mathbf{S}(\mathbf{V}_p(\mathbf{r}_{p,j,Gauss})) + \mathbf{I}(\mathbf{r})$$

where the g_js are the weights of the Gaussian quadrature method and the points $\mathbf{r}_{p,j,Gauss}$ are chosen according to the Gauss quadrature formula. It is to be noted that the choice of a particular quadrature formula can make a huge difference in accuracy and computing time, see appendix A.2.

Having chosen the type of quadrature we solve with Banach's theorem:

$$\mathbf{V}_h^f = \mathbf{W}_h \cdot \mathbf{S}(\mathbf{V}_h^f) + \mathbf{I}_h, \tag{17}$$

i.e., we compute the fixed point at the level of approximation defined by h.

The following theorem ensures that $\lim_{h\to 0} \mathbf{V}_h^f = \mathbf{V}^f$:

Theorem 5.2 *Assume that* $\lim_{h\to 0} \mathbf{W}_h = \mathbf{W}$ *in* $\mathbf{L}^2_{n\times n}(\Omega\times\Omega)$, *then* $\max_{1\le j\le \lfloor \frac{1}{h} \rfloor} |\mathbf{V}_h(\mathbf{r}_{h,j}) - \mathbf{V}^f(\mathbf{r}_{h,j})| = O(a_h) \xrightarrow{h} 0$ *with* $a_h = \|\mathbf{W} - \mathbf{W}_h\|_F$

Proof. The proof is an adaptation of [34, Theorem 19.5]. □

5.2 Examples of bumps

We show four examples of the application of the previous numerical method to the computation of bumps for various values of n and q.

There are n populations ($\mathbf{V} = [V_1, \cdots, V_n]^T$, $\mathbf{W} \in \mathbf{L}^2_{n\times n}(\Omega\times\Omega)$), some excitatory and some inhibitory. $\Omega = [-1, 1]^q$. We characterize in section 6.2 how the shape of Ω influences that of the bumps. The connectivity matrix is of the form

$$W_{ij}(\mathbf{r},\, \mathbf{r}') = \alpha_{ij} \exp\left(-\frac{1}{2} \left\langle \mathbf{r} - \mathbf{r}', \mathbf{T}_{ij} (\mathbf{r} - \mathbf{r}') \right\rangle\right), \tag{18}$$

with $\mathbf{T}_{ij} \in \mathcal{M}_{q\times q}$ is a $q \times q$ symmetric positive definite matrix. The weights α_{ij}, $i, j = 1, \cdots, n$ form an element $\boldsymbol{\alpha}$ of $\mathcal{M}_{n\times n}$ and $\mathbf{T} = \begin{bmatrix} \mathbf{T}_{11} & \mathbf{T}_{12} \\ \mathbf{T}_{21} & \mathbf{T}_{22} \end{bmatrix}$ is an element of $\mathcal{M}_{nq\times nq}$. The weights $\boldsymbol{\alpha}$ are chosen so that $DS_m \|\mathbf{W}\|_F < 1$. The sign

of α_{ij}, $i \neq j$, indicates whether population j excites or inhibits population i. The bumps are computed using the algorithm described in the previous section.

First example: $n = 2,\ q = 2$**, constant current**

Figure 3 shows an example of a bump for the following values of the parameters:

$$\boldsymbol{\alpha} = \begin{bmatrix} 0.2 & -0.1 \\ 0.1 & -0.2 \end{bmatrix} \quad \mathbf{I} = [-0.3,\ 0]^T \quad \mathbf{T} = \begin{bmatrix} 40 & 0 & 12 & 0 \\ 0 & 40 & 0 & 12 \\ 8 & 0 & 20 & 0 \\ 0 & 8 & 0 & 20 \end{bmatrix}$$

There is one excitatory and one inhibitory population of neural masses.

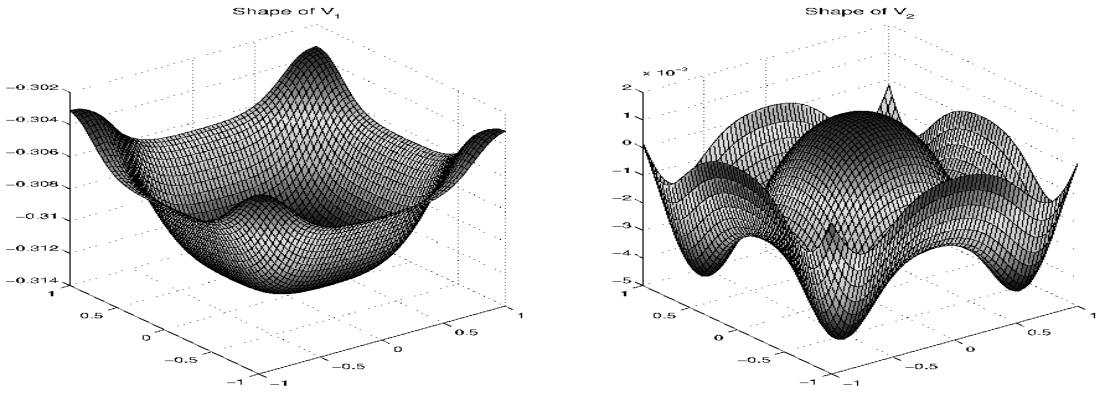

Fig. 3. Example of a two-population, two-dimensional bump with constant external currents (see text).

Second example: $n = 2,\ q = 2$**, non constant current**

Figure 4 shows a different example where the external current $\mathbf{I}$ is still equal to 0 for its second coordinate and is not constant but equal to its previous value, -0.3 to which we have added a circularly symmetric 2D Gaussian centered at the point of coordinates $(0.5,\ 0,5)$ of the square Ω with standard deviation 0.18 and maximum value 0.2. It is interesting to see how the shape of the previous bump is perturbed. The matrix $\boldsymbol{\alpha}$ is the same as in the first example. The matrix $\mathbf{T}$ is equal to

$$\mathbf{T} = \begin{bmatrix} 5 & 0 & 1 & 0 \\ 0 & 5 & 0 & 1 \\ 16 & 0 & 40 & 0 \\ 0 & 16 & 0 & 40 \end{bmatrix},$$

corresponding to a spatially broader interaction for the first population and narrower for the second.

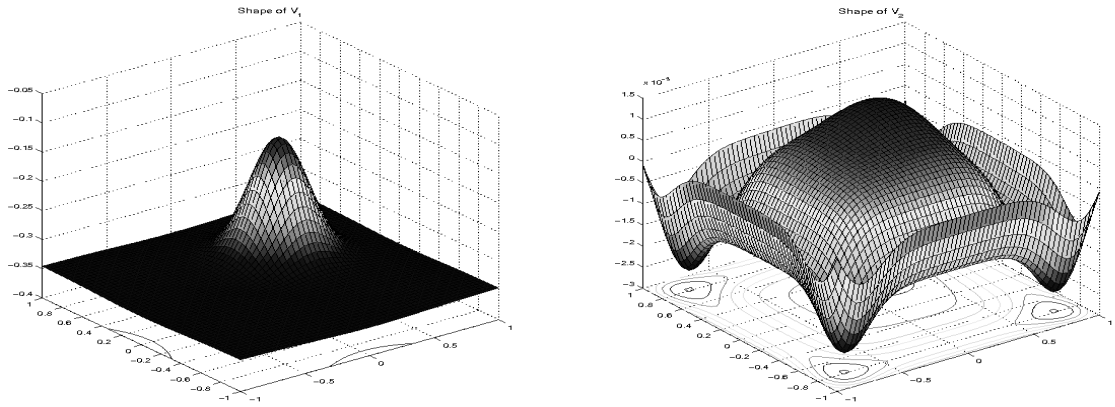

Fig. 4. Example of a two-population, two-dimensional bump with Gaussian shaped external current (see text).

Third example: $n = 3,\ q = 2$**, constant current**

Figure 5 shows an example of a bump for three neural populations, two excitatory and one inhibitory, in two dimensions. We use the following values of the parameters:

$$\boldsymbol{\alpha} = \begin{bmatrix} .442 & 1.12 & -0.875 \\ 0 & 0.1870 & -0.0850 \\ 0.128 & 0.703 & -0.7750 \end{bmatrix}^T \qquad \mathbf{I} = [0,\ 0]^T \qquad \mathbf{T} = \begin{bmatrix} 40 & 0 & 12 & 0 & 12 & 0 \\ 0 & 40 & 0 & 12 & 0 & 12 \\ 8 & 0 & 20 & 0 & 9 & 0 \\ 0 & 8 & 0 & 20 & 0 & 9 \\ 40 & 0 & 12 & 0 & 12 & 0 \\ 0 & 40 & 0 & 12 & 0 & 12 \end{bmatrix}$$

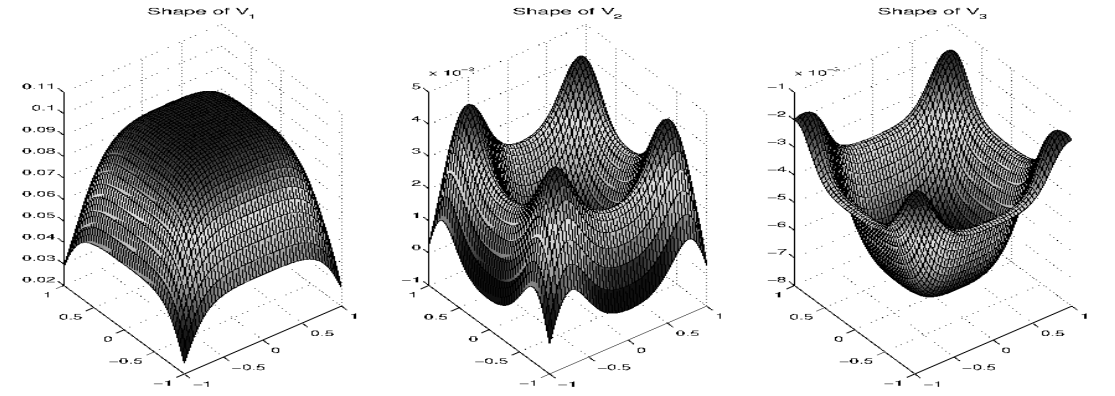

Fig. 5. Example of a three-population, two-dimensional bump (see text).

Fourth example: $n = 2$, $q = 3$**, constant current** We show an example of a 3-dimensional bump for two populations of neural masses. The parameters are:

$$\boldsymbol{\alpha} = \begin{bmatrix} 0.2 & -0.1 \\ 0.1 & -0.2 \end{bmatrix} \quad \mathbf{I} = [0,\ 0]^T \quad \mathbf{T} = \begin{bmatrix} 40\,\mathrm{Id}_3 & 12\,\mathrm{Id}_3 \\ 8\,\mathrm{Id}_3 & 20\,\mathrm{Id}_3 \end{bmatrix},$$

where Id_3 is the 3×3 identity matrix.

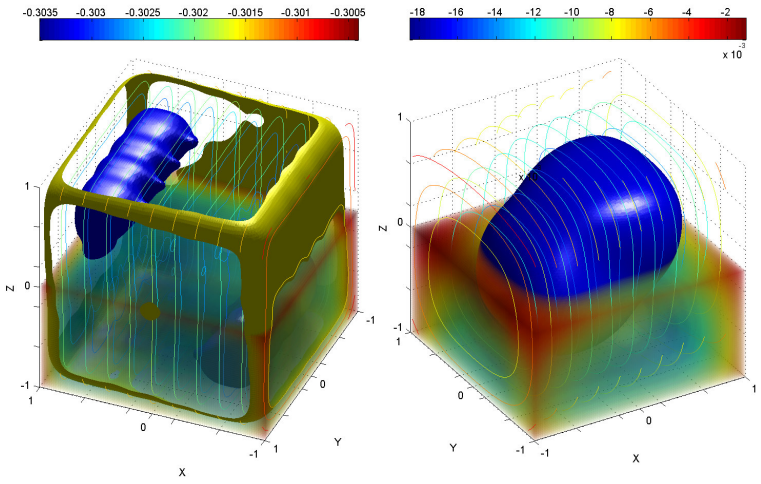

Fig. 6. Example of a two-population, three-dimensional bump, isosurfaces are shown. Transparencies increases linearly from red to blue.

6 Sensitivity of the bump to variations of the parameters

In this section we characterize how the solutions of (9) vary with the parameters that appear in the equation. These parameters are of two types: first we have a finite number of real parameters such as the external currents, the weights in the connectivity matrix $\mathbf{W}$, or the parameters of the sigmoids, and, second, the shape of the domain Ω, a potentially infinite-dimensional parameter.

We focus on the voltage-based model, the analysis in the activity-based case is very similar. We start with a set of general considerations in the finite dimensional case which we then apply to the various cases. We then tackle the more difficult case of the dependency with respect to the shape of Ω.

As f_v is a smooth function of the parameters ($\mathbf{I}$, $\boldsymbol{\alpha}$, $\mathbf{S}\ldots$), one can show (by extending Banach's theorem) that the fixed point $\mathbf{V}^f$ inherits the smoothness of f_v.

We introduce the linear operator [2] $\mathbf{W} \cdot D\mathbf{S}(\mathbf{V}^f) : \mathcal{F} \to \mathcal{F}$ such that

$$\mathbf{W} \cdot D\mathbf{S}(\mathbf{V}^f) \cdot \mathbf{V}(\mathbf{r}) = \int_\Omega \mathbf{W}(\mathbf{r},\, \mathbf{r}') D\mathbf{S}(\mathbf{V}^f(\mathbf{r}'))\mathbf{V}(\mathbf{r}')\, d\mathbf{r}' \quad \forall \mathbf{V} \in \mathcal{F}$$

We have the following

Proposition 6.1 *The derivative $\partial_\lambda \mathbf{V}^f$ of the fixed point $\mathbf{V}^f$ with respect to the generic parameter λ satisfies the equation*

$$(\mathrm{Id} - \mathbf{W} \cdot D\mathbf{S}(\mathbf{V}^f)) \cdot \partial_\lambda \mathbf{V}^f = \mathbf{b}(\lambda, \mathbf{V}^f), \tag{19}$$

where $\mathbf{b}(\lambda, \mathbf{V}^f) = (\partial_\lambda \mathbf{W}) \cdot \mathbf{S}(\mathbf{V}^f) + \mathbf{W} \cdot (\partial_\lambda \mathbf{S}(\mathbf{V}^f)) + \partial_\lambda \mathbf{I}$.

Proof. Taking the derivative of both sides of (16) with respect to λ, we have:

$$\partial_\lambda \mathbf{V}^f = \mathbf{W} \cdot D\mathbf{S}(\mathbf{V}^f) \cdot \partial_\lambda \mathbf{V}^f + (\partial_\lambda \mathbf{W}) \cdot \mathbf{S}(\mathbf{V}^f) + \mathbf{W} \cdot (\partial_\lambda \mathbf{S}(\mathbf{V}^f)) + \partial_\lambda \mathbf{I},$$

hence we obtain equation (19). □

Note that $\partial_\lambda \mathbf{S}(\mathbf{V}^f)$ is the partial derivative of the vector $\mathbf{S}$ with respect to the scalar parameter λ evaluated at $\mathbf{V} = \mathbf{V}^f$.

Because of the assumption $DS_m \|\mathbf{W}\|_F < 1$ the linear operator $\mathbf{J} = \mathrm{Id} - \mathbf{W} \cdot D\mathbf{S}(\mathbf{V}^f)$ is invertible with

$$\mathbf{J}^{-1} = \sum_{p=0}^{\infty} \left(\mathbf{W} \cdot D\mathbf{S}(\mathbf{V}^f)\right)^p,$$

and the series is convergent.

$\partial_\lambda \mathbf{V}^f$ is thus obtained from the following formula

$$\partial_\lambda \mathbf{V}^f = \mathbf{J}^{-1} \mathbf{b}(\lambda, \mathbf{V}^f),$$

the righthand side being computed by

$$\begin{cases} x_0 &= \mathbf{b}(\lambda, \mathbf{V}^f) \\ x_{p+1} &= x_0 + \mathbf{W} \cdot D\mathbf{S}(\mathbf{V}^f) \cdot x_p \quad p \geq 0 \end{cases}$$

We now apply proposition 6.1 to the study of the sensitivity of the bump to the variations of the parameters.

[2] $\mathbf{W} \cdot D\mathbf{S}(\mathbf{V}^f)$ is the Frechet derivative of the operator f_v at the point $\mathbf{V}^f$ of $\mathcal{F}$.

6.1.1 Sensitivity of the bump to the exterior current

When $\lambda = I_1$, we find:

$$\partial_{I_1} \mathbf{V}^f = \mathbf{J}^{-1} \begin{bmatrix} 1 \\ 0 \end{bmatrix} \geq \begin{bmatrix} 0 \\ 0 \end{bmatrix}$$

This inequality is to be understood component by component. It predicts the influence of I_1 on $\mathbf{V}^f$. For example, with the parameters $\boldsymbol{\alpha}$ and $\mathbf{T}$ used in figure 3 but with an external current equal to 0, we obtain the bump shown in figure 7 (top) with the derivatives shown at the bottom of the same figure. We also show in figure 8 of V_1 and V_2 along the diagonal and the x-axis for different values of I_1 close to 0. The reader can verify that the values increase with I_1, as predicted.

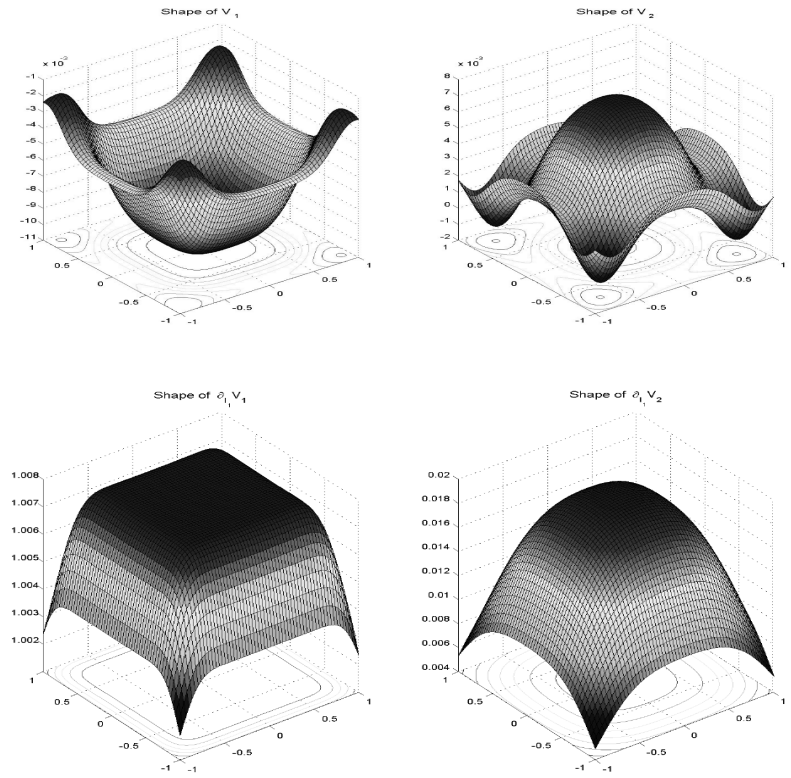

Fig. 7. A bump corresponding to the following parameters $\boldsymbol{\alpha}$ and $\mathbf{T}$ are the same as in figure 3, $I = [0\ 0]^T$ (top). Derivative of the bump with respect to the first coordinate, I_1, of the exterior current (bottom). We verify that it is positive (see text).

6.1.2 Sensitivity of the bump to the weights $\boldsymbol{\alpha}$

For $\lambda = \alpha_{ij}$, one finds:

$$\mathbf{J} \cdot \partial_{\alpha_{ij}} \mathbf{V}^f = \partial_{\alpha_{ij}} \mathbf{W} \cdot D\mathbf{S}(\mathbf{V}^f)$$

We then have

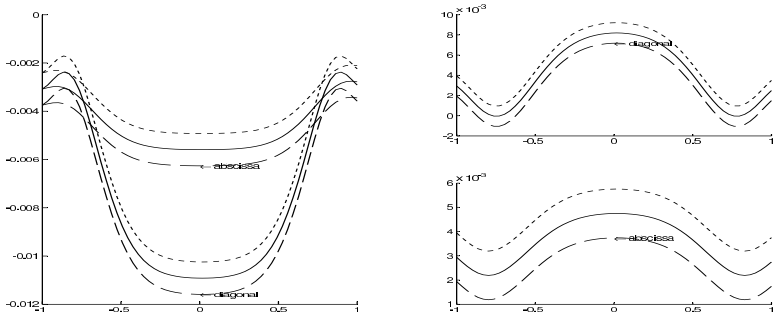

Fig. 8. Cross sections of V_1 (left) and V_2 (right) for $I_1 = -0.001$ (green), $I_1 = 0$ (black) and $I_1 = 0.001$ (blue). $I_2 = 0$ in all three cases. To increase the readibility of the results we have applied an offset of 0.001 and 0.002 to the black and blue curves on the righthand side of the figure, respectively.

$\lambda = a$: We find

$$\partial_a \mathbf{V}^f(\mathbf{r}) = \mathbf{J}^{-1} \cdot \begin{bmatrix} \exp\left(-\frac{1}{2}\left\langle \mathbf{r}-\cdot,\, \mathbf{T}_{11}\left(\mathbf{r}-\cdot\right)\right\rangle\right) & 0 \\ 0 & 0 \end{bmatrix} \cdot D\mathbf{S}(\mathbf{V}^f) =$$

$$\mathbf{J}^{-1} \cdot \begin{bmatrix} \exp\left(-\frac{1}{2}\left\langle \mathbf{r}-\cdot, \mathbf{T}_{11}\left(\mathbf{r}-\cdot\right)\right\rangle S_1'(V_1^f(\cdot))\right) \\ 0 \end{bmatrix} \geq \begin{bmatrix} 0 \\ 0 \end{bmatrix}$$

The fixed point is an increasing function of the excitatory parameter a.

$\lambda = b$: We find

$$\partial_b \mathbf{V}^f(\mathbf{r}) = \mathbf{J}^{-1} \cdot \begin{bmatrix} 0 & -\exp\left(-\frac{1}{2}\left\langle \mathbf{r}-\cdot, \mathbf{T}_{12}\left(\mathbf{r}-\cdot\right)\right\rangle\right) \\ 0 & 0 \end{bmatrix} \cdot D\mathbf{S}(\mathbf{V}^f) =$$

$$\mathbf{J}^{-1} \cdot \begin{bmatrix} -\exp\left(-\frac{1}{2}\left\langle \mathbf{r}-\cdot, \mathbf{T}_{12}\left(\mathbf{r}-\cdot\right)\right\rangle\right) S_2'(V_2^f(\cdot)) \\ 0 \end{bmatrix} \leq \begin{bmatrix} 0 \\ 0 \end{bmatrix}$$

The fixed point is a decreasing function of the inhibitory parameter b, see figure 9.

The other cases are similar.

6.1.3 Sensitivity of the bump to the thresholds

When $\lambda = \theta_i,\ i = 1,\ 2$ we have from the definition (15) of $\mathbf{S}$ and with the notations of proposition 6.1:

$$\mathbf{b}(\lambda,\, \mathbf{V}^f) = -\mathbf{W} \cdot D\mathbf{S}(\mathbf{V}^f) \cdot \mathbf{e}_i,\ i = 1,\ 2,$$

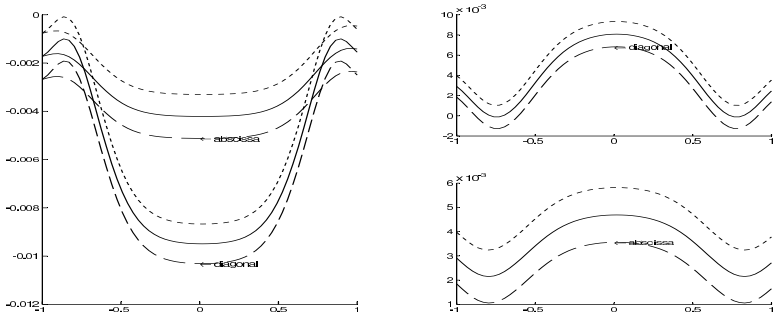

Fig. 9. Cross sections of V_1 (left) and V_2 (right) for $b = -0.101$ (green), $b = -0.1$ (black) and $b = -0.099$ (blue). To increase the readibility of the results we have applied an offset of 0.001 and $+0.002$ to all black and blue curves, respectively.

where $\mathbf{e}_1 = [1,\, 0]^T$, $\mathbf{e}_2 = [0,\, 1]^T$. We show in figure 10 some cross sections of the bump $\mathbf{V}^f$ obtained for the same values of the parameters as in figure 3 and three values of the threshold vector.

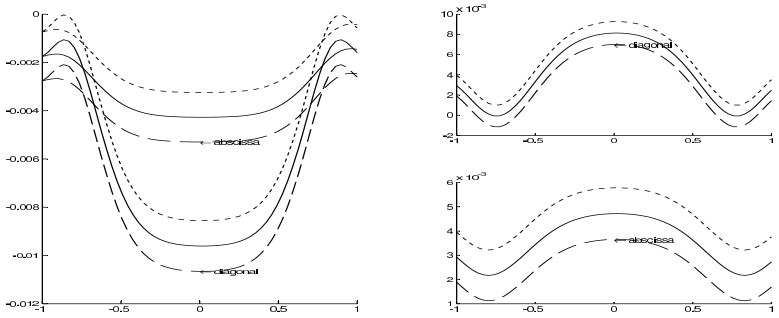

Fig. 10. Cross sections of V_1 (left) and V_2 (right) for $\boldsymbol{\theta} = -0.101[1,\, 1]^T$ (green), $\boldsymbol{\theta} = 0$ (black) and $\boldsymbol{\theta} = 0.1[1,\, 1]^T$ (blue). To increase the readibility of the results we have applied an offset of 0.001 and $+0.002$ to all black and blue curves, respectively.

6.1.4 Sensitivity of the bump to the slope of the sigmoid

When $\lambda = s_i,\ i = 1,\, 2$ we have from the definition (15) of $\mathbf{S}$ and with the notations of proposition 6.1:

$$\mathbf{b}(\lambda,\, \mathbf{V}^f) = \mathbf{W} \cdot D\mathbf{S}(\mathbf{V}^f) \cdot \mathbf{s}\left(\mathbf{V}^f - \boldsymbol{\theta}\right),$$

where the matrix $\mathbf{s}$ is given by

$$\mathbf{s} = \begin{bmatrix} \frac{1}{s_1} & 0 \\ 0 & \frac{1}{s_2} \end{bmatrix}$$

Figure 11 shows the two coordinates $\partial_s V_1^f$ and $\partial_s V_2^f$ for $s_1 = s_2 = s$ of the derivative of the bump $\mathbf{V}^f$ at $s = 1$ obtained for the same values of the other parameters as in figure 3, except the intensity which is equal to 0.

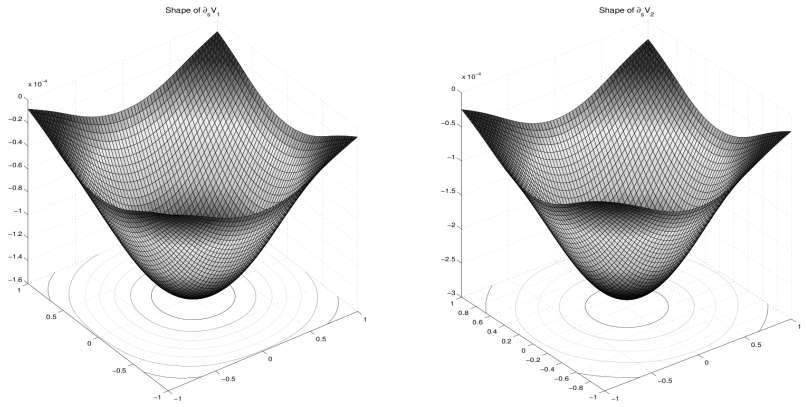

Fig. 11. Plot of the derivative with respect to the slope of the sigmoids of the the bump obtained with the same parameters $\boldsymbol{\alpha}$, $\mathbf{I}$ and $\mathbf{T}$ as in figure 3.

6.2 Sensitivity of the bump to variations of the shape of the domain Ω

We expect the bump to be somewhat dependent on the shape of Ω. It would nonetheless be desirable that this dependency would not be too strong for the modeling described in this paper to have some biological relevance. Indeed, if the bumps are metaphores of persistent states, we expect them to be relatively robust to the actual shape of the cortical part being modeled. For example if we take Ω to be a representation of the primary visual cortex $V1$ whose shape varies from individual to individual it would come as a surprise if the shape of a bump induced by the same spatially constant stimulus would be drastically different.

Technically, in order to study the dependence of $\mathbf{V}^f$ with respect to Ω we need to assume that Ω is smooth, i.e. its border $\partial\Omega$ is a smooth curve ($q = 2$) or surface ($q = 3$) unlike the previous examples where Ω was the square $[-1, 1]^2$. But even a difficulty arises from the fact that the set of regular domains is not a vector space, hence the derivative of a function (the bump) with respect to a domain has to be defined with some care. The necessary background is found in appendix A.3.

We make explicit the fact that the connectivity function $\mathbf{W}$ has been normalized to satisfy $\|\mathbf{W}\|_F = 1$ by writing $\mathbf{W}(\mathbf{r},\, \mathbf{r}',\, \Omega)$ where, with some abuse of notation

$$\mathbf{W}(\mathbf{r},\, \mathbf{r}',\, \Omega) = \mathbf{W}(\mathbf{r},\, \mathbf{r}')/J(\Omega) \quad \text{with} \quad J(\Omega) = \sqrt{\int_{\Omega\times\Omega} \|\mathbf{W}(\mathbf{r},\, \mathbf{r}')\|_F^2 \, d\mathbf{r}\, d\mathbf{r}'}$$

Theorem 6.2 *Let us assume that Ω is a smooth bounded domain of $\mathbb{R}^q$. If $\mathbf{W}$ is in $\mathbf{W}^{1,2}_{n\times n}(\Omega\times\Omega)$, $\mathbf{I}_{\rm ext}$ is in $\mathbf{W}^{1,2}_n(\Omega)$ (see appendix A.1 for a definition) the material derivative (see appendix A.3 for a definition) $\mathbf{V}^f_m(\mathbf{r},\,\Omega)$ of the bump $\mathbf{V}^f$ satisfies the following equation:*

$$\mathbf{V}^f_m(\mathbf{r},\Omega,\mathbf{X}) = \int_\Omega \mathbf{W}(\mathbf{r},\,\mathbf{r}',\,\Omega)D\mathbf{S}\Big(\mathbf{V}^f(\mathbf{r}',\Omega)\Big)\mathbf{V}^f_m(\mathbf{r}',\Omega,\mathbf{X})\,d\mathbf{r}' \tag{20}$$

$$+\int_\Omega \mathbf{W}(\mathbf{r},\mathbf{r}',\,\Omega)\mathbf{S}\Big(\mathbf{V}^f(\mathbf{r}',\Omega)\Big)div\mathbf{X}(\mathbf{r}')d\mathbf{r}' \tag{21}$$

$$+\int_\Omega D_1\mathbf{W}(\mathbf{r},\mathbf{r}',\,\Omega)\mathbf{X}(\mathbf{r})\mathbf{S}\Big(\mathbf{V}^f(\mathbf{r}',\Omega)\Big)d\mathbf{r}' \tag{22}$$

$$+\int_\Omega D_2\mathbf{W}(\mathbf{r},\mathbf{r}',\,\Omega)\mathbf{X}(\mathbf{r}')\mathbf{S}\Big(\mathbf{V}^f(\mathbf{r}',\Omega)\Big)d\mathbf{r}' \tag{23}$$

$$-\frac{\langle J'(\Omega),\,\mathbf{X}\rangle}{J(\Omega)}\Big(\mathbf{V}^f(\mathbf{r},\,\Omega)-\mathbf{I}_{\rm ext}(\mathbf{r})\Big)+D\mathbf{I}_{\rm ext}(\mathbf{r})\cdot\mathbf{X}(\mathbf{r}) \tag{24}$$

where D_i, $i=1,\,2$ indicates the derivative with respect to the ith variable and $\langle J'(\Omega),\,\mathbf{X}\rangle$ is the Gâteaux derivative of $J(\Omega)$ with respect to the vector field $\mathbf{X}$:

$$\langle J'(\Omega),\,\mathbf{X}\rangle = \lim_{\tau\to 0}\frac{J(\Omega(\tau))-J(\Omega)}{\tau},$$

where $\mathbf{X}$ is defined in the proof below. We have

$$\langle J'(\Omega),\,\mathbf{X}\rangle = \frac{1}{2J(\Omega)}\Big(\int_{\Omega\times\partial\Omega}\|\mathbf{W}(\mathbf{r},\,\mathbf{r}',\,\Omega)\|^2_F\,\langle\mathbf{X}(\mathbf{r}'),\,\mathbf{N}(\mathbf{r}')\rangle\,d\mathbf{r}\,d\mathbf{a}(\mathbf{r}')+$$
$$\int_{\partial\Omega\times\Omega}\|\mathbf{W}(\mathbf{r},\,\mathbf{r}',\,\Omega)\|^2_F\,\langle\mathbf{X}(\mathbf{r}'),\,\mathbf{N}(\mathbf{r}')\rangle\,d\mathbf{a}(\mathbf{r})\,d\mathbf{r}'\Big),$$

where $d\mathbf{a}$ is the surface element on the smooth boundary $\partial\Omega$ of Ω, and $\mathbf{N}$ its unit inward normal vector.

Proof. The proof uses ideas that are developed in [12],
[48], see also the appendix A.3. We want to compute :

$$\mathbf{V}^f_m(\mathbf{r},\,\Omega,\,\mathbf{X}) = \lim_{\tau\to 0}\frac{\mathbf{V}^f(\mathbf{r}(\tau),\,\Omega(\tau))-\mathbf{V}^f(\mathbf{r},\,\Omega)}{\tau}$$

from equation (9). As far as the computation of the derivative is concerned only small deformations are relevant and we consider the first order Taylor expansion of the transformation T:

$$T(\tau,\,\mathbf{r}) = T(0,\,\mathbf{r})+\tau\frac{\partial T}{\partial\tau}(0,\,\mathbf{r}) = \mathbf{r}+\tau\mathbf{X}(\mathbf{r})$$

We define:

$$\begin{aligned}\Delta \equiv \frac{1}{\tau}\Big(&\int_{\Omega(\tau)} \mathbf{W}(\mathbf{r}(\tau), \mathbf{r}',\, \Omega(\tau))\mathbf{S}(\mathbf{V}^f(\mathbf{r}', \Omega(\tau)))d\mathbf{r}' \\ &- \int_{\Omega} \mathbf{W}(\mathbf{r}, \mathbf{r}',\, \Omega)\mathbf{S}(\mathbf{V}^f(\mathbf{r}', \Omega))\, d\mathbf{r}' \\ &+ \mathbf{I}_{\text{ext}}(\mathbf{r} + \tau\mathbf{X}(r)) - \mathbf{I}_{\text{ext}}(\mathbf{r})\Big)\end{aligned}$$

In the first integral, we make the change of variable $\mathbf{r}' \to \mathbf{r}' + \tau\mathbf{X}$ and obtain:

$$\frac{1}{\tau}\int_{\Omega} \mathbf{W}(\mathbf{r}+\tau\mathbf{X}(\mathbf{r}), \mathbf{r}'+\tau\mathbf{X}(\mathbf{r}'),\, \Omega+\tau\mathbf{X})\mathbf{S}(\mathbf{V}^f(\mathbf{r}'+\tau\mathbf{X}(\mathbf{r}'), \Omega+\tau\mathbf{X}))|\mathrm{det}J_\tau(\mathbf{r}')|d\mathbf{r}'$$

We have :

$$\mathrm{det}J_\tau(\mathbf{r}') = 1 + \tau\mathrm{div}(\mathbf{X}(\mathbf{r}')) + o(\tau).$$

Hence for τ sufficiently small $\mathrm{det}J_\tau > 0$. Moreover:

$$\lim_{\tau\to 0} \mathrm{det}J_\tau = 1 \quad \lim_{\tau\to 0} \frac{\mathrm{det}J_\tau(\mathbf{r}') - 1}{\tau} = \mathrm{div}(\mathbf{X}(\mathbf{r}')),$$

and

$$\begin{aligned}\mathbf{W}(\mathbf{r} + \tau\mathbf{X}(\mathbf{r}), \mathbf{r}' + \tau\mathbf{X}(\mathbf{r}'),\, \Omega + \tau\mathbf{X}) = \\ \mathbf{W}(\mathbf{r}, \mathbf{r}') + \tau D_1\mathbf{W}(\mathbf{r}, \mathbf{r}')\mathbf{X}(\mathbf{r}) + \tau D_2\mathbf{W}(\mathbf{r}, \mathbf{r}')\mathbf{X}(\mathbf{r}') \\ - \tau\frac{\langle J'(\Omega),\, \mathbf{X}\rangle}{J(\Omega)}\mathbf{W}(\mathbf{r},\, \mathbf{r}',\, \Omega) + o(\tau),\end{aligned}$$

where D_i, $i = 1, 2$ indicates the derivative with respect to the ith argument. Thus we have:

$$\begin{aligned}\tau\Delta = &\int_{\Omega} \mathbf{W}(\mathbf{r}, \mathbf{r}',\, \Omega)\Big(\mathbf{S}(\mathbf{V}^f(\mathbf{r}' + \tau\mathbf{X}(\mathbf{r}'), \Omega + \tau\mathbf{X})) - \mathbf{S}(\mathbf{V}^f(\mathbf{r}', \Omega))\Big)\mathrm{det}J_\tau(\mathbf{r}')d\mathbf{r}' \\ &+ \int_{\Omega} \mathbf{W}(\mathbf{r}, \mathbf{r}',\, \Omega)\mathbf{S}(\mathbf{V}^f(\mathbf{r}', \Omega))\Big(\mathrm{detJ}_\tau(\mathbf{r}') - 1\Big)d\mathbf{r}' \\ &+ \tau\Big\{ \int_{\Omega} D_1\mathbf{W}(\mathbf{r}, \mathbf{r}',\, \Omega)\mathbf{X}(\mathbf{r})\mathbf{S}(\mathbf{V}^f(\mathbf{r}' + \tau\mathbf{X}(\mathbf{r}'), \Omega + \tau\mathbf{X}))\mathrm{detJ}_\tau(\mathbf{r}')d\mathbf{r}' \\ &+ \int_{\Omega} D_2\mathbf{W}(\mathbf{r}, \mathbf{r}',\, \Omega)\mathbf{X}(\mathbf{r}')\mathbf{S}(\mathbf{V}^f(\mathbf{r}' + \tau\mathbf{X}(\mathbf{r}'), \Omega + \tau\mathbf{X}))\mathrm{detJ}_\tau(\mathbf{r}')d\mathbf{r}' \\ &- \frac{\langle J'(\Omega),\, \mathbf{X}\rangle}{J(\Omega)} \int_{\Omega} \mathbf{W}(\mathbf{r}, \mathbf{r}',\, \Omega)\mathbf{S}(\mathbf{V}^f(\mathbf{r}' + \tau\mathbf{X}(\mathbf{r}'), \Omega + \tau\mathbf{X}))\mathrm{detJ}_\tau(\mathbf{r}')d\mathbf{r}' \\ &+ D\mathbf{I}_{\text{ext}}(\mathbf{r}) \cdot \mathbf{X}(\mathbf{r})\Big\}\end{aligned}$$

Because

$$\lim_{\tau\to 0} \frac{\mathbf{S}(\mathbf{V}^f(\mathbf{r}' + \tau\mathbf{X}(\mathbf{r}'), \Omega + \tau\mathbf{X})) - \mathbf{S}(\mathbf{V}^f(\mathbf{r}', \Omega))}{\tau} = D\mathbf{S}(\mathbf{V}^f(\mathbf{r}', \Omega))\mathbf{V}^f_m(\mathbf{r}', \Omega, \mathbf{X}),$$

and $\int_\Omega \mathbf{W}(\mathbf{r},\, \mathbf{r}',\, \Omega)\mathbf{S}\Big(\mathbf{V}^f(\mathbf{r}', \Omega)\Big)\, d\mathbf{r}' \,=\, \mathbf{V}^f(\mathbf{r},\, \Omega) - \mathbf{I}_{\text{ext}}(\mathbf{r})$, we obtain equation (20). The value of $\langle J'(\Omega),\, \mathbf{X}\rangle$ is obtained from corollary A.8. □

Equation (20) is of the same form as before:

$$\begin{aligned}(\mathbf{J}\cdot\mathbf{V}_m^f)(\mathbf{r},\Omega,\mathbf{X}) = &\int_\Omega \mathbf{W}(\mathbf{r},\mathbf{r}',\,\Omega)\mathbf{S}\Big(\mathbf{V}^f(\mathbf{r}',\Omega)\Big) div\mathbf{X}(\mathbf{r}')d\mathbf{r}'\\ &+\int_\Omega D_1\mathbf{W}(\mathbf{r},\mathbf{r}',\,\Omega)\mathbf{X}(\mathbf{r})\mathbf{S}\Big(\mathbf{V}^f(\mathbf{r}',\Omega)\Big)d\mathbf{r}'\\ &+\int_\Omega D_2\mathbf{W}(\mathbf{r},\mathbf{r}',\,\Omega)\mathbf{X}(\mathbf{r}')\mathbf{S}\Big(\mathbf{V}^f(\mathbf{r}',\Omega)\Big)d\mathbf{r}'\\ &-\frac{\langle J'(\Omega),\,\mathbf{X}\rangle}{J(\Omega)}(\mathbf{V}^f(\mathbf{r},\,\Omega)-\mathbf{I}_{\text{ext}}(\mathbf{r}))\end{aligned}$$

This result tells us that the shape of the bump varies smoothly with respect to the shape of the domain Ω.

6.2.1 Numerical application for the domain derivatives

We show in figure 12 the bump $\mathbf{V}^f$ for Ω equal to the unit disc $D(0,1)$ and in figure 13 the one for Ω equal to the ellipse [3] $Ellipse(1.2,1)$ of equation $\frac{r_1^2}{a^2}+r_2^2-1=0$. The values of the weight parameters $\boldsymbol{\alpha}$ are the same as in figure 3 and $\mathbf{I}=[0,\,0]^T$. The matrix $\mathbf{T}$ is equal to

$$\mathbf{T}=\begin{bmatrix}40 & 0 & 10 & 0\\ 0 & 10 & 0 & 12\\ 12 & 0 & 40 & 0\\ 0 & 40 & 0 & 40\end{bmatrix}$$

Note that because the diagonal elements are not equal for T_{11}, T_{12} and T_{13}, $\mathbf{W}$ is not circularly symmetric and so is the bump in figure 12 despite the fact that Ω is circularly symmetric.

Finally we show in figure 14 the two coordinates of the shape (material) derivative of the first bump in the direction of the field $\mathbf{X}$ corresponding to the transformation

$$T(\tau,\,\mathbf{r})=\mathbf{r}+\tau\begin{bmatrix}(a-1)r_1\\ 0\end{bmatrix}$$

$T(1)$ transforms the disc $D(0,1)$ into the ellipse $Ellipse(a,1)$, $\mathbf{X}(\mathbf{r}) = [(a-1)r_1,\,0]^T$.

[3] $Ellipse(a,\,b)$ represents the ellipse lying along the first axis of coordinates with semi-major axis a and semiminor axis b.

Thus $div\mathbf{X} = (a-1)$ and, because of (18):

$$(\mathbf{J}\cdot\mathbf{V}_m^f)(\mathbf{r},\Omega,\mathbf{X}) = \Big(a-1-\frac{\langle J'(\Omega),\,\mathbf{X}\rangle}{J(\Omega)}\Big)\Big(\mathbf{V}^f-\mathbf{I}\Big)+ \int_\Omega D_1\mathbf{W}(\mathbf{r},\mathbf{r}',\,\Omega)\Big(\mathbf{X}(\mathbf{r})-\mathbf{X}(\mathbf{r}')\Big)\mathbf{S}\Big(\mathbf{V}^f(\mathbf{r}',\Omega)\Big)d\mathbf{r}',$$

and

$$\langle J'(\Omega),\,\mathbf{X}\rangle = \frac{\int_{\Omega\times\partial\Omega}\|\mathbf{W}(\mathbf{r},\,\mathbf{r}',\,\Omega)\|_F^2\,\langle\mathbf{X}(\mathbf{r}'),\,\mathbf{N}(\mathbf{r}')\rangle\;d\mathbf{r}\,d\mathbf{a}(\mathbf{r}')}{J(\Omega)}$$

As the Gaussian quadrature formula holds for a rectangular domain, we use polar coordinates to map the disk (or the ellipse) to a square. For our numerical study we can simplify these expressions (the matrixes $\mathbf{T}_{ij}$ are symmetric) :

$$\Big[\int_\Omega D_1\mathbf{W}(\mathbf{r},\mathbf{r}',\,\Omega)\Big(\mathbf{X}(\mathbf{r})-\mathbf{X}(\mathbf{r}')\Big)\mathbf{S}\Big(\mathbf{V}^f(\mathbf{r}',\Omega)\Big)d\mathbf{r}'\Big]_i =$$
$$\sum_j\int_\Omega\Big(\mathbf{r}-\mathbf{r}'\Big)^T\mathbf{T}_{ij}\Big(\mathbf{X}(\mathbf{r})-\mathbf{X}(\mathbf{r}')\Big)W_{ij}(\mathbf{r},\mathbf{r}',\,\Omega)S_j\Big(V_j^f(\mathbf{r}',\Omega)\Big)d\mathbf{r}'\;\;i=1,\cdots,n$$

Thus we can use a simple modification of the algorithm that computes $\mathbf{W}\cdot\mathbf{S}(\mathbf{V})$ to obtain the previous expression.

$J(\Omega)$ and $\langle J'(\Omega),\,\mathbf{X}\rangle$ are computed with a Gauss quadrature formula. For a circle in polar coordinates $\mathbf{N}(\mathbf{r}') = \mathbf{r}'$.

Let us be a bit more precise. In the case showed in figure 12, we choose $\mathbf{I} = 0$. Using Banach's theorem we compute $\mathbf{V}_{Gauss}^f$ for $N = 30$ and use Nyström's interpolation to compute $\mathbf{V}_{Nys}^f$ for $n = 100$ (for example) points on each axis.

Then, using $\mathbf{V}_{Gauss}^f$, we compute $\mathbf{V}_{m,Gauss}^f$ for N points. But the equation for $\mathbf{V}_m^f$ reads:

$$\mathbf{V}_m^f = \mathbf{W}.D\mathbf{S}(\mathbf{V}^f).\mathbf{V}_m^f + \langle J'(\Omega),\,\mathbf{X}\rangle$$

Having computed a Nyström interpolation of n points for $\mathbf{V}_m^f = \mathbf{W}.D\mathbf{S}(\mathbf{V}^f).\mathbf{V}_m^f + \langle J'(\Omega),\,\mathbf{X}\rangle$, we again use a Nyström interpolation with the last equation to compute $\mathbf{V}_{m,Nystrom}^f$ for n points on each axis.

We used this numerical method in every previous example related to the computation of derivatives.

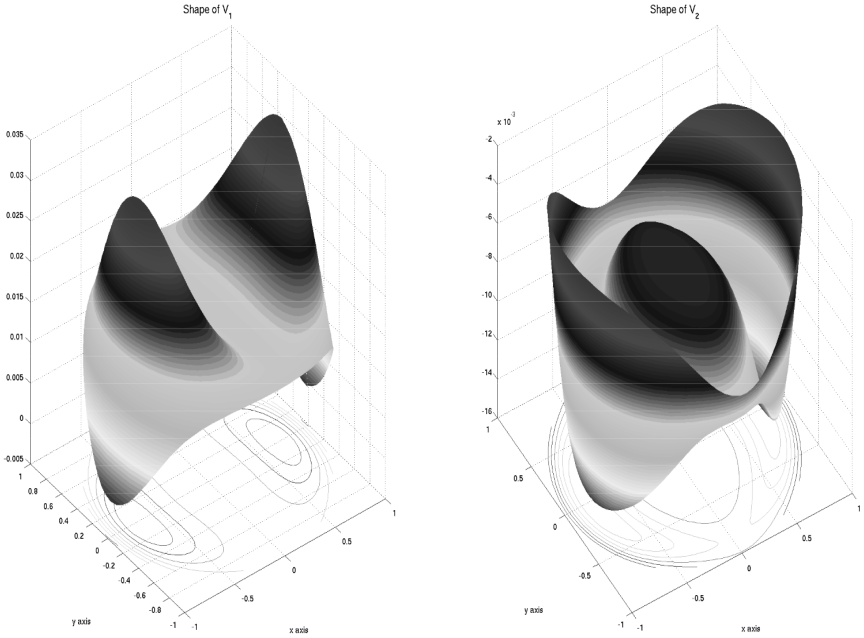

Fig. 12. The unit disk and its bump $\mathbf{V}^f$.

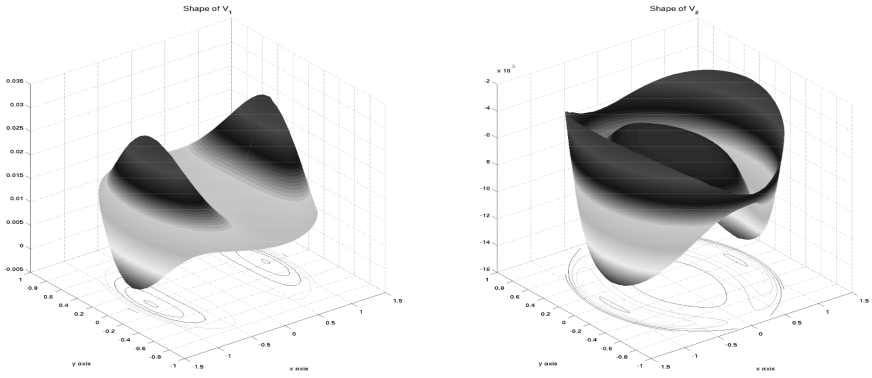

Fig. 13. Bump associated to the ellipse with major axis along the r_1 coordinate and the minor axis along the r_2 coordinate. The ratio of the axes length is $a = 1.2$, see text.

7 Conclusion and perspectives

We have studied two classes (voltage- and activity-based) of neural continuum networks in the context of modeling macroscopic parts of the cortex. In both cases we have assumed an arbitrary number of interacting neuron populations, either excitatory or inhibitory. These populations are spatially related by non-symmetric connectivity functions representing cortico-cortical, local, connections. External inputs are also present in our models to represent non-local connections, e.g., with other cortical areas. The relationship between (average) membrane potential and activity

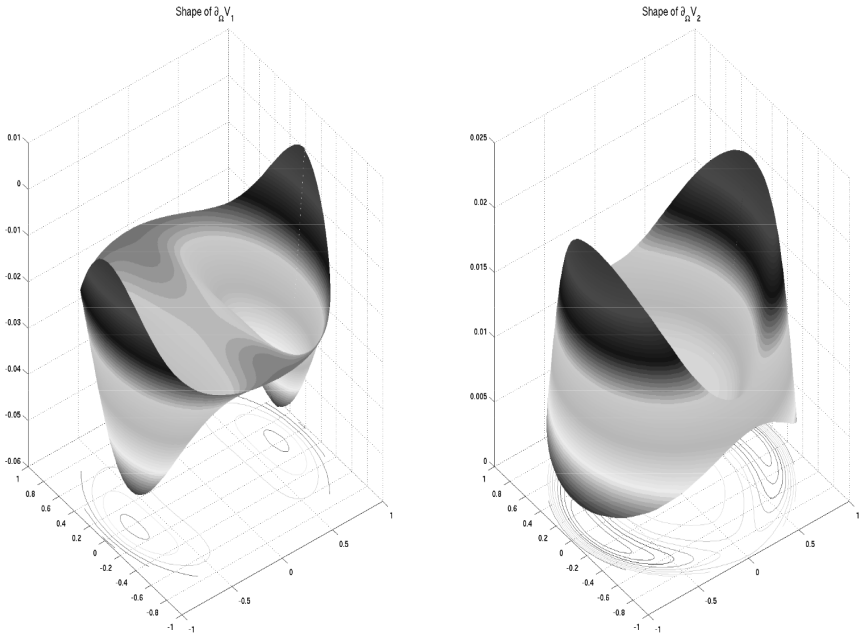

Fig. 14. The shape derivative $\mathbf{V}_m^f$ for $a = 1.2$.

is described by nondegenerate sigmoidal nonlinearities, i.e., not by Heaviside functions which have often been considered instead in the literature because of their (apparent) simplicity.

The resulting nonlinear integro-differential equations are of the Hammerstein type [27] and generalise those proposed by Wilson and Cowan
[56].

Departing from most of the previous work in this area we relax the usual assumption that the domain of definition where we study these networks is infinite, i.e. equal to $\mathbb{R}$ or $\mathbb{R}^2$ and we explicitely consider the biologically much more relevant case of a bounded subset Ω of $\mathbb{R}^q$, $q = 1,\ 2,\ 3$, obviously a better model of a piece of cortex.

Using methods of functional analysis, we have studied the existence and uniqueness of a stationary, i.e., time-independent, solution of these equations in the case of a stationary input. These solutions are often referred to as persistent states, or bumps, in the literature.

We have proved that, under very mild assumptions on the connectivity functions, such solutions always exist (this is due in part to the fact that we do not use Heaviside functions).

We have provided sufficient conditions on the connectivity functions for the solution to be absolutely stable, that is to say independent of the initial state of the

network. These conditions can be expressed in terms of the spectra of some functional operators, that we prove to be compact, that arise very naturally from the equations describing the network activity.

We have also studied the sensitivity of the solution(s) to variations of such parameters as the connectivity functions, the sigmoids, the external inputs, and the shape of the domain of definition of the neural continuum networks. This last analysis is more involved than the others because of the infinite dimensional nature of the shape parameter. An analysis of the bifurcations of the solutions when the parameters vary over large ranges requires the use of techniques of bifurcation analysis for infinite dimensional systems and is out of the scope of this paper.

We believe and we hope by now to have convinced the reader that the functional analysis framework that we have used in this paper is the right one to try and answer some of the mathematical questions that are raised by models of connected networks of nonlinear neurons. We also believe that some of these also begin to answer biological questions since these networks models, despite the admitedly immense simplifications they are built from, are nonetheless metaphores of real neural assemblies.

A Notations and background material

A.1 Matrix norms and spaces of functions

We note $\mathcal{M}_{n\times n}$ the set of $n \times n$ real matrixes. We consider the Frobenius norm on $\mathcal{M}_{n\times n}$

$$\|\mathbf{M}\|_F = \sqrt{\sum_{i,j=1}^{n} M_{ij}^2},$$

and consider the space $\mathbf{L}^2_{n\times n}(\Omega \times \Omega)$ of the functions from $\Omega \times \Omega$ to $\mathcal{M}_{n\times n}$ whose Frobenius norm is in $L^2(\Omega \times \Omega)$. If $\mathbf{W} \in \mathbf{L}^2_{n\times n}(\Omega \times \Omega)$ we note $\|\mathbf{W}\|_F^2 = \int_{\Omega\times\Omega} \|\mathbf{W}(\mathbf{r}, \mathbf{r}')\|_F^2 \, d\mathbf{r}\, d\mathbf{r}'$. Note that this implies that each element W_{ij}, $i, j = 1, \cdots, n$ in in $L^2(\Omega \times \Omega)$. We note $\mathcal{F}$ the set $\mathbf{L}^2_n(\Omega)$ of square-integrable mappings from Ω to $\mathbb{R}^n$ and $\|\mathbf{x}\|_{\mathcal{F}}$ the corresponding norm. We have the following

Lemma A.1 *Given* $\mathbf{x} \in \mathbf{L}^2_n(\Omega)$ *and* $\mathbf{W} \in \mathbf{L}^2_{n\times n}(\Omega \times \Omega)$*, we define* $\mathbf{y}(\mathbf{r}) = \int_\Omega \mathbf{W}(\mathbf{r}, \mathbf{r}')\mathbf{x}(\mathbf{r}')\, d\mathbf{r}'$*. This integral is well defined for almost all* $\mathbf{r}$*,* $\mathbf{y}$ *is in* $\mathbf{L}^2_n(\Omega)$ *and we have*

$$\|\mathbf{y}\|_{\mathcal{F}} \leq \|\mathbf{W}\|_F \, \|\mathbf{x}\|_{\mathcal{F}}.$$

Proof. Since each W_{ij} is in $L^2(\Omega\times\Omega)$, $W_{ij}(\mathbf{r}, .)$ is in $L^2(\Omega)$ for almost all $\mathbf{r}$, thanks to Fubini's theorem. So $W_{ij}(\mathbf{r}, .)x_j(.)$ is integrable for almost all $\mathbf{r}$ from what we

deduce that $\mathbf{y}$ is well-defined for almost all $\mathbf{r}$. Next we have

$$|y_i(\mathbf{r})| \leq \sum_j \left| \int_\Omega W_{ij}(\mathbf{r}, \mathbf{r}')\, x_j(\mathbf{r}')\, d\mathbf{r}' \right|$$

and (Cauchy-Schwarz):

$$|y_i(\mathbf{r})| \leq \sum_j \left(\int_\Omega W_{ij}^2(\mathbf{r}, \mathbf{r}')\, d\mathbf{r}' \right)^{1/2} \|x_j\|_2,$$

from where it follows that (Cauchy-Schwarz again, discrete version):

$$|y_i(\mathbf{r})| \leq \left(\sum_j \|x_j\|_2 2 \right)^{1/2} \left(\sum_j \int_\Omega W_{ij}^2(\mathbf{r}, \mathbf{r}')\, d\mathbf{r}' \right)^{1/2} = \|\mathbf{x}\|_{\mathcal{F}} \left(\sum_j \int_\Omega W_{ij}^2(\mathbf{r}, \mathbf{r}')\, d\mathbf{r}' \right)^{1/2},$$

from what it follows that $\mathbf{y}$ is in $\mathbf{L}_n^2(\Omega)$ (thanks again to Fubini's theorem) and

$$\|\mathbf{y}\|_{\mathcal{F}}^2 \leq \|\mathbf{x}\|_{\mathcal{F}}^2 \sum_{i,j} \int_{\Omega\times\Omega} W_{ij}^2(\mathbf{r}, \mathbf{r}')\, d\mathbf{r}'\, d\mathbf{r} = \|\mathbf{x}\|_{\mathcal{F}}^2 \|\mathbf{W}\|_F^2.$$

□

We also use the following

Lemma A.2 *For each $\mathbf{V}$ of $\mathcal{F}$, $\mathbf{S}(\mathbf{V})$ is in $\mathcal{F}$ and we have*

$$\|\mathbf{S}(\mathbf{V})\|_{\mathcal{F}} \leq S_m \sqrt{n|\Omega|}$$

For all $\mathbf{V}_1$ and $\mathbf{V}_2$ in $\mathcal{F}$ we have

$$\|\mathbf{S}(\mathbf{V}_1) - \mathbf{S}(\mathbf{V}_2)\|_{\mathcal{F}} \leq DS_m \|\mathbf{V}_1 - \mathbf{V}_2\|_{\mathcal{F}},$$

where DS_m is defined in Definition 2.1.

Proof. We have $\|\mathbf{S}(\mathbf{V})\|_{\mathcal{F}}^2 = \sum_{i=1}^n \int_\Omega (S_i(V_i(\mathbf{r})))^2\, d\mathbf{r} \leq S_m^2 n|\Omega|$, where $|\Omega|$ is the Lebesgue measure of Ω (its area). Similarly, $\|\mathbf{S}(\mathbf{V}_1) - \mathbf{S}(\mathbf{V}_2)\|_{\mathcal{F}}^2 = \sum_{i=1}^n \int_\Omega (S_i(V_i^1(\mathbf{r})) - S_i(V_i^2(\mathbf{r})))^2\, d\mathbf{r} \leq (DS_m)^2 \sum_{i=1}^n \int_\Omega (V_i^1(\mathbf{r}) - V_i^2(\mathbf{r}))^2\, d\mathbf{r} = (DS_m)^2 \|\mathbf{V}_1 - \mathbf{V}_2\|_{\mathcal{F}}^2$ □
In theorem 6.2 we use the Sobolev spaces $\mathbf{W}_n^{1,2}(\Omega)$ and $\mathbf{W}_{n\times n}^{1,2}(\Omega \times \Omega)$. $\mathbf{W}_n^{1,2}(\Omega)$ is the set of functions $\mathbf{X} : \Omega \to \mathbb{R}^n$ such that each component X_i, $i = 1, \cdots, n$ is in $W^{1,2}(\Omega)$, the set of functions of $L^2(\Omega)$ whose first order derivatives exist in the weak sense and are also in $L^2(\Omega)$ (see [16]). Similarly $\mathbf{W}_{n\times n}^{1,2}(\Omega \times \Omega)$ is the set of functions $\mathbf{X} : \Omega \to \mathcal{M}_{n\times n}$ such that each component X_{ij}, $i, j = 1, \cdots, n$ is in is in $W^{1,2}(\Omega)$.

A.2 Choice of the quadrature method

We emphasize the importance of the choice of a specific quadrature formula using the following example : $\int_{-1}^{1} e^{-t}dt = e - 1/e$ where we compare a 0th-order finite elements methods with and Gauss' method (the parameters of the Gauss quadrature formula are computed with a precision of 10^{-16} using Newton's method).

Method	Value
Exact	2.350 402 387 287 603...
0th-order (N=1000)	2.351 945...
finite element	
Gauss (N=5)	2.350 402 386 46...

The Gauss method is far more powerful and allows us to compute bumps in 3D for an arbitrary number of populations.

A.3 Shape derivatives

As it has already been pointed out, the computation of the variation of the bump with respect to the shape of the region Ω is difficult since the set $\mathcal{U}$ of regular domains (regular open bounded sets) of $\mathbb{R}^q$ does not have the structure of a vector space. Variations of a domain must then defined in some way. Let us consider a reference domain $\Omega \in \mathcal{U}$ and the set $\mathcal{A}$ of aplications $T : \Omega \to \mathbb{R}^q$ which are at least as regular as homeomorphisms, i.e. one to one with T and T^{-1} one to one. In detail

$$\mathcal{A} = \left\{ T \text{ one to one, } T,\, T^{-1} \in W^{1,\infty}(\Omega, \mathbb{R}^q) \right\},$$

where the functional space $W^{1,\infty}(\Omega, \mathbb{R}^q)$ is the set of mappings such that they and their first order derivatives are in $L^\infty(\Omega,\, \mathbb{R}^q)$. In detail

$$W^{1,\infty}(\Omega, \mathbb{R}^q) = \{T : \Omega \to \mathbb{R}^q \text{ such that } T \in L^\infty(\Omega,\, \mathbb{R}^q) \text{ and } \partial_i T \in L^\infty(\Omega,\, \mathbb{R}^q),\, i = 1, \cdots, q\}$$

Given a shape function $F : \mathcal{U} \to \mathbb{R}^q$, for $T \in \mathcal{A}$, let us define $\hat{F}(T) = F(T(\Omega))$. The key point is that since $W^{1,\infty}(\Omega, \mathbb{R}^q)$ is a Banach space we can define the notion of a derivative with respect to the domain Ω as

Definition A.3 *F is Gâteaux differentiable with respect to Ω if and only if $\hat{F}$ is Gâteaux differentiable with respect to T.*

In order to compute Gâteaux derivatives with respect to T we introduce a family of deformations $(T(\tau))_{\tau \geq 0}$ such that $T(\tau) \in \mathcal{A}$ for $\tau \geq 0$, $T(0) = Id$, and

$T(\cdot) \in C^1([0,\, A];\, W^{1,\infty}(\Omega, \mathbb{R}^q))$, $A > 0$. From a practical point of view, there are many ways to construct such a family, the most famous one being the Hadamard deformation [25] which goes as follows.

For a point $\mathbf{r} \in \Omega$ we note

$$\mathbf{r}(\tau) = T(\tau,\, \mathbf{r}) \;\text{ with }\; T(0, \mathbf{r}) = \mathbf{r}$$
$$\Omega(\tau) = T(\tau,\, \Omega) \text{ with } T(0, \Omega) = \Omega)$$

Let us now define the velocity vector field $\mathbf{X}$ corresponding to $T(\tau)$ as

$$\mathbf{X}(\mathbf{r}) = \frac{\partial T}{\partial \tau}(0,\, \mathbf{r}) \quad \forall \mathbf{r} \in \Omega$$

From definition A.3 follows the

Definition A.4 *The Gâteaux derivative of a shape function $F(\Omega)$ in the direction of $\mathbf{X}$, denoted $\langle F'(\Omega),\, \mathbf{X}\rangle$, is equal to*

$$\langle F'(\Omega),\, \mathbf{X}\rangle = \lim_{\tau \to 0} \frac{F(\Omega(\tau)) - F(\Omega)}{\tau}$$

We also introduce the

Definition A.5 *The material derivative of a function $f(\mathbf{r},\, \Omega)$, noted $f_m(\mathbf{r},\, \Omega,\, \mathbf{X})$ is defined by*

$$f_m(\mathbf{r},\, \Omega,\, \mathbf{X}) = \lim_{\tau \to 0} \frac{\mathbf{V}(\mathbf{r}(\tau),\, \Omega(\tau)) - \mathbf{V}(\mathbf{r},\, \Omega)}{\tau},$$

and

Definition A.6 *The shape derivative of a function $f(\mathbf{r},\, \Omega)$, noted $f_s(\mathbf{r},\, \Omega,\, \mathbf{X})$ is defined by*

$$f_s(\mathbf{r},\, \Omega,\, \mathbf{X}) = \lim_{\tau \to 0} \frac{f(\mathbf{r},\, \Omega(\tau)) - f\mathbf{r},\, \Omega)}{\tau},$$

The following theorem whose proof can be found, e.g., in [12], [48] relates the Gâteaux derivative and the shape derivative

Theorem A.7 *The Gâteaux derivative of the functional $F(\Omega) = \int_\Omega f(\mathbf{r}, \Omega)\, d\mathbf{r}$ in the direction of $\mathbf{X}$ is given by*

$$\langle F'(\Omega),\, \mathbf{X}\rangle = \int_\Omega f_s(\mathbf{r},\, \Omega,\, \mathbf{X})\, d\mathbf{r} - \int_{\partial\Omega} f(\mathbf{r},\, \Omega)\, \langle \mathbf{X}(\mathbf{r}),\, \mathbf{N}(\mathbf{r})\rangle\, d\mathbf{a}(\mathbf{r}),$$

where $\mathbf{N}$ is the unit inward normal to $\partial\Omega$ and $d\mathbf{a}$ its area element.

The following corollary is used in the proof of theorem 6.2.

Corollary A.8 *The Gâteaux derivative of the functional* $F(\Omega) = \int_\Omega f(\mathbf{r})\, d\mathbf{r}$ *in the direction of* $\mathbf{X}$ *is given by*

$$\langle F'(\Omega),\, \mathbf{X}\rangle = -\int_{\partial\Omega} f(\mathbf{r})\ \langle \mathbf{X}(\mathbf{r}),\, \mathbf{N}(\mathbf{r})\rangle\ d\mathbf{a}(\mathbf{r}),$$

where $\mathbf{N}$ *is the unit inward normal to* $\partial\Omega$ *and* $d\mathbf{a}$ *its area element.*

References

[1] S.-I. Amari. Dynamics of pattern formation in lateral-inhibition type neural fields. *Biological Cybernetics*, 27(2):77–87, jun 1977.

[2] J. Appell and C.-J Chen. How to solve Hammerstein equations. *Journal of integral equations and applications*, 18(3):287–296, 2006.

[3] P. Blomquist, J. Wyller, and G.T. Einevoll. Localized activity patterns in two-population neuronal networks. *Physica D*, 206:180–212, 2005.

[4] P. Bressloff. Spontaneous symmetry breaking in self–organizing neural fields. *Biological Cybernetics*, 93(4):256–274, oct 2005.

[5] D.P. Buxhoeveden and M.F. Casanova. The minicolumn hypothesis in neuroscience. *Brain*, 125:935–951, 2002.

[6] L. M. Chalupa and J.S. Werner, editors. *The visual neurosciences*. MIT Press, 2004.

[7] C.L. Colby, J.R. Duhamel, and M.E. Goldberg. Oculocentric spatial representation in parietal cortex. *Cereb. Cortex*, 5:470–481, 1995.

[8] Stephen Coombes. Waves, bumps, and patterns in neural fields theories. *Biological Cybernetics*, 93(2):91–108, 2005.

[9] Olivier David, Diego Cosmelli, and Karl J. Friston. Evaluation of different measures of functional connectivity using a neural mass model. *NeuroImage*, 21:659–673, 2004.

[10] Olivier David and Karl J. Friston. A neural mass model for meg/eeg: coupling and neuronal dynamics. *NeuroImage*, 20:1743–1755, 2003.

[11] P. Dayan and L. F. Abbott. *Theoretical Neuroscience : Computational and Mathematical Modeling of Neural Systems*. MIT Press, 2001.

[12] M.C. Delfour and J.-P. Zolésio. *Shapes and geometries*. Advances in Design and Control. Siam, 2001.

[13] Jean Dieudonné. *Foundations of Modern Analysis*. Academic Press, 1960.

[14] K. Doubrovinski. Dynamics, stability and bifurcation phenomena in the nonlocal model of cortical activity. U.u.d.m. project report 2005:8, Uppsala University, Department of Mathematics, jun 2005.

[15] Bard Ermentrout. Neural networks as spatio-temporal pattern-forming systems. *Reports on Progress in Physics*, 61:353–430, 1998.

[16] L.C. Evans. *Partial Differential Equations*, volume 19 of *Graduate Studies in Mathematics*. Proceedings of the American Mathematical Society, 1998.

[17] O. Faugeras, F. Grimbert, and J.J. Slotine. Stability and synchronization in neural fields. In *Sixteenth Annual Computational Neuroscience Meeting (CNS)*, jul 2007.

[18] W.J. Freeman. Mass action in the nervous system. *Academic Press, New York*, 1975.

[19] S. Funahashi, C.J. Bruce, and P.S. Goldman-Rakic. Mnemonic coding of visual space in the monkey's dorsolateral prefrontal cortex. *J. Neurophysiol.*, 61:331–349, 1989.

[20] W. Gerstner and W. M. Kistler. Mathematical formulations of hebbian learning. *Biological Cybernetics*, 87:404–415, 2002.

[21] F. Grimbert and O. Faugeras. Bifurcation analysis of Jansen's neural mass model. *Neural Computation*, 18(12):3052–3068, December 2006.

[22] Y. Guo and C.C. Chow. Existence and stability of standing pulses in neural networks: Ii stability. *SIAM Journal on Applied Dynamical Systems*, 4:249–281, 2005.

[23] Yixin Guo and Carson C. Chow. Existence and stability of standing pulses in neural networks: I. existence. *SIAM Journal on Applied Dynamical Systems*, 4(2):217–248, 2005.

[24] B.S. Gutkin, G.B. Ermentrout, and J. O'Sullivan. Layer 3 patchy recurrent excitatory connections may determine the spatial organization of sustained activity in the primate prefrontal cortex. *Neurocomputing*, 32-33:391–400, 2000.

[25] J. Hadamard. Mémoire sur un problème d'analyse relatif à l'équilibre des plaques élastiques encastrées. *Mémoire des savants étrangers*, 1968. CNRS, Paris.

[26] Stefan Haeusler and Wolfgang Maass. A statistical analysis of information-processing properties of lamina-specific cortical microcircuits models. *Cerebral Cortex*, 17:149–162, jan 2007.

[27] A. Hammerstein. Nichtlineare integralgleichungen nebst anwendungen. *Acta Math.*, 54:117–176, 1930.

[28] Michiel Hazewinkel, editor. *Encyclopaedia of Mathematics*. Springer, 2001.

[29] J. J. Hopfield. Neurons with graded response have collective computational properties like those of two-state neurons. *Proceedings of the National Academy of Sciences, USA*, 81(10):3088–3092, 1984.

[30] F.C. Hoppenstaedt and E.M. Izhikevich. *Weakly Connected Neural Networks*. Springer-Verlag, New York, 1997.

[31] Ben H. Jansen and Vincent G. Rit. Electroencephalogram and visual evoked potential generation in a mathematical model of coupled cortical columns. *Biological Cybernetics*, 73:357–366, 1995.

[32] Ben H. Jansen, George Zouridakis, and Michael E. Brandt. A neurophysiologically-based mathematical model of flash visual evoked potentials. *Biological Cybernetics*, 68:275–283, 1993.

[33] E.R. Kandel, J.H. Schwartz, and T.M. Jessel. *Principles of Neural Science*. McGraw-Hill, 4th edition, 2000.

[34] M.A. Krasnosel'skii, G.M. Vainikko, P.P. Zabreiko, and V.Ya. Stetsenko. *Approximate solutions of operator equations*. Wolteers-Noordhoff, 1972. Translated by D. Louvish.

[35] C.L. Laing, W.C. Troy, B. Gutkin, and G.B. Ermentrout. Multiple bumps in a neuronal model of working memory. *SIAM J. Appl. Math.*, 63(1):62–97, 2002.

[36] C.R. Laing and W.C. Troy. Two-bump solutions of amari-type models of neuronal pattern formation. *Physica D*, 178(3):190–218, apr 2003.

[37] F.H. Lopes da Silva, W Blanes, S.N. Kalitzin, J. Parra, P. Suffczynski, and D.N. Velis. Dynamical diseases of brain systems: different routes to epileptic seizures. *IEEE transactions in biomedical ingeneering*, 50(5):540–548, 2003.

[38] F.H. Lopes da Silva, A. Hoeks, and L.H. Zetterberg. Model of brain rhythmic activity. *Kybernetik*, 15:27–37, 1974.

[39] F.H. Lopes da Silva, A. van Rotterdam, P. Barts, E. van Heusden, and W. Burr. Model of neuronal populations. the basic mechanism of rhythmicity. *M.A. Corner, D.F. Swaab (eds) Progress in brain research, Elsevier, Amsterdam*, 45:281–308, 1976.

[40] Kiyotoshi Matsuoka. Stability conditions for nonlinear continuous neural networks with asymmetric connection weights. *Neural Networks*, 5:495–500, 1992.

[41] E.K. Miller, C.A. Erickson, and R. Desimone. Neural mechanisms of visual working memory in prefrontal cortex of the Macaque. *J. Neurosci.*, 16:5154–5167, 1996.

[42] V.B. Mountcastle. Modality and topographic properties of single neurons of cat's somatosensory cortex. *Journal of Neurophysiology*, 20:408–434, 1957.

[43] V.B. Mountcastle. The columnar organization of the neocortex. *Brain*, 120:701–722, 1997.

[44] D.J. Pinto and G.B. Ermentrout. Spatially structured activity in synaptically coupled neuronal networks: 1. traveling fronts and pulses. *SIAM J. of Appl. Math.*, 62:206–225, 2001.

[45] D.J. Pinto and G.B. Ermentrout. Spatially structured activity in synaptically coupled neuronal networks: 2. standing pulses. *SIAM J. of Appl. Math.*, 62:226–243, 2001.

[46] William H. Press, Brian P. Flannery, Saul A. Teukolsky, and William T. Vetterling. *Numerical Recipes in C*. Cambridge University Press, 1988.

[47] J.E. Rubin and W.C. Troy. Sustained spatial patterns of activity in neuronal populations without recurrent excitation. *SIAM journal on applied mathematics*, 64(5):1609–1635, 2004.

[48] J. Sokolowski and J.-P. Zolésio. *Introduction to shape optimization. Shape sensitivity analysis.*, volume 16 of *Springer Ser. Comput. Math.* Springer-Verlag, Berlin, 1992.

[49] J. Stoer and R. Bulirsch. *Introduction to Numerical Analysis*. Springer-Verlag, 1972.

[50] Alex M. Thomson and A. Peter Bannister. Interlaminar connections in the neocortex. *Cerebral Cortex*, 13:5–14, January 2003.

[51] F.G. Tricomi. *Integral Equations*. Dover, 1985. Reprint.

[52] A. van Rotterdam, F.H. Lopes da Silva, J. van den Ende, M.A. Viergever, and A.J. Hermans. A model of the spatial-temporal characteristics of the alpha rhythm. *Bulletin of Mathematical Biology*, 44(2):283–305, 1982.

[53] F. Wendling, F. Bartolomei, JJ. Bellanger, and P. Chauvel. Interpretation of interdependencies in epileptic signals using a macroscopic physiological model of the eeg. *Clinical Neurophysiology*, 112(7):1201–1218, 2001.

[54] F. Wendling, J.J. Bellanger, F. Bartolomei, and P. Chauvel. Relevance of nonlinear lumped-parameter models in the analysis of depth-eeg epileptic signals. *Biological Cybernetics*, 83:367–378, 2000.

[55] Herrad Werner and Tim Richter. Circular stationary solutions in two-dimensional neural fields. *Biological Cybernetics*, 85(3):211–217, sep 2001.

[56] H.R. Wilson and J.D. Cowan. A mathematical theory of the functional dynamics of cortical and thalamic nervous tissue. *Biological Cybernetics*, 13(2):55–80, sep 1973.